PERGAMON

Quaternary Science Reviews 20 (2001) 1623–1647

QSR

Sand sheet dynamics and Quaternary landscape evolution of the Selima Sand Sheet, southern Egypt

Ted A. Maxwell[a,*], C. Vance Haynes Jr.[b,c]

[a]*Center for Earth and Planetary Studies, National Air and Space Museum, Smithsonian Institution, Washington, DC 20560 USA*
[b]*Department. of Anthropology, University of Arizona, Tucson, AZ 85721 USA*
[c]*Department of Geosciences, University of Arizona, Tucson, AZ 85721 USA*

Abstract

The Selima Sand Sheet occupies more than 120,000 km^2 of the hyperarid, uninhabited Darb el-Arba'in Desert centered at the border of Egypt and Sudan at latitude 22° N, and is characterized by a featureless surface of lag granules and fine sand broken only by widely separated dune fields and giant ripples of varying height and wavelength. Monitoring of the largest of these chevron-shaped ripples using repeat orbital images and field surveys indicates migration rates of 500–1000 m/yr, accompanied by 0–2.0 cm erosion or deposition of the youngest sand sheet stratigraphic units. Beneath this active surface, several developmental stages of sand sheet sediments have undulatory upper contacts and varying degrees of pedogenic alteration. The younger stages retain their horizontal lamination and have cracking patterns indicative of past wetter conditions, while older stages have lost their laminar structure through pedogenesis. Historical remains in the desert as well as ^{14}C and Uranium-series dating indicate that the younger strata of the sand sheet have a very low accumulation rate, despite the active movement of the surface. The lower strata were extensively modified during mid and late Pleistocene pluvials, resulting in an initial undulatory surface that set the stage for later accumulation of sand sheet. Below these Quaternary sediments lies irregular topography dissected by channels of mid-Tertiary drainage. The Selima Sand Sheet is neither the result of net aggradation nor degradation, but results from inheritance of an initial fluvial landscape increasingly modified during climatic cycles. Wet periods led to local drainage and deposition, while the increasingly severe arid periods of the late Pleistocene and Holocene resulted in deposition of the blanketing bimodal sediments of the sand sheet.

1. Introduction

The present-day surface of western Egypt consists of a broad sloping monocline that dips gently to the north, floored by middle to late mesozoic, continental- to shallow-marine sediments in the south and early Tertiary marine sequences in the north (Issawi, 1972). This surface is broken by south-facing scarps that outline the major depressions in the Western desert, the Kharga-Dakhla oases, and the Bahariya depression 300 km north of Kharga (Fig. 1). South of these widely separated oases, the mesozoic sequence is covered by active aeolian deposits and quaternary soils and is known as the Darb el-Arba'in Desert after the 40-day camel caravan track that crosses the eastern part of the desert (Haynes, 1982a). The Selima Sand Sheet occupies the central part of the Darb el-Arba'in Desert, and was interpreted as a broad aeolian peneplain by Sandford (1933). The southern portion of the sand sheet was traversed numerous times by the Sudan Defense Force, supplying Kufra Oasis in Libya from Sudan during World War II (Wright, 1945), but was not studied during that period because of the bland nature of the surface. Some idea of the surface characteristics can be inferred from its description by Bagnold (1990, p. 66):

A single utterly flat sheet of firm sand, it is now known to cover an area of nearly 100,000 square miles. Driving at speed for hour after hour, on a compass bearing, often blindly into a mirage, it became hard to stay awake. On one occasion both occupants of a car did fall asleep, the driver's foot remaining hard down on the pedal. They were only retrieved after an anxious chase.

Both the similarity of the surface to that of Mars (El-Baz et al., 1980; El-Baz and Maxwell, 1982) and the discovery of subsurface channels via the Shuttle Imaging

* Corresponding author. Tel.: + 1-202-357-2767; fax: + 1-202-633-8926.
E-mail address: tmaxwell@nasm.si.edu (T.A. Maxwell).

0277-3791/01/$ - see front matter
PII: S0277-3791(01)00009-9

Radar experiments (McCauley et al., 1982) prompted remote sensing studies of the sand sheet in the past two decades. The few scattered, uninhabited oases in the region had long been the sites of archaeological expeditions, from which has come most of our knowledge of the nature and timing of climate change in southern Egypt (Wendorf et al., 1976; Wendorf and Schild, 1980; Said, 1980; Haynes, 1982b; Pachur et al., 1987).

Hypotheses for the development of the sand sheet range from aeolian to fluvial mechanisms. Sandford (1933) and Peel (1966) attributed the origin of the sand sheet to the penultimate stage of erosion of the desert surface, and interpreted the widely scattered relict hills north and south of the region as outliers left by aeolian deflation. Haynes (1982a) proposed that climatic cycling was most important, suggesting that climate change alternately weakened the bedrock surface during humid periods, which made them susceptible to aeolian erosion during arid cycles. Even before the identification of subsurface channels with spaceborne radar, Breed et al. (1982) had proposed the existence of a now-extinct river system that originated in the remaining highlands of the Gilf Kebir Plateau west of the sand sheet and had eroded the surface, now taken over by aeolian sculpturing.

The discovery of channels buried beneath the sand sheet in the Shuttle Imaging Radar A (SIR-A) experiment led to renewed interest in the Tertiary history of the region (McCauley et al., 1982), the location of archaeological sites (McHugh et al., 1988, 1989), and the evolution of north African drainage. The few channel junctions present in the radar images suggested to McCauley et al. (1986) a southwestward drainage direction, away from the present Nile valley although this hypothesis has not been universally accepted (Burke and Wells, 1989). According to Issawi and McCauley (1992), the latest Tertiary channels were deflected by the uplift of the Gilf Kebir plateau region, and drained into the Mediterranean through central Egypt. It was not until the desiccation of the Mediterranean during the late miocene that the present channel of the Nile was deepened in response to this new, lower base level (Said, 1990, p. 506). Whether early generations of Nile drainage were supported by channels entering the Nile valley south of Aswan from the west, or whether those channels of the Darb el-Arba'in Desert were captured by the newly incised Nile is open to conjecture (Said, 1993, p. 37). In either case, it is apparent that several generations of fluvial deposits are (or were) present in the area of the Selima Sand Sheet (Haynes et al., 1993), which are now visible only through radar imaging or at the surface by the geographic patterns of sandstone and limestone outcrops east of the sand sheet.

The purpose of this paper is to present the results of monitoring the sand sheet between 1987 and 1999 both in the field and by use of orbital images. This has been done to establish present-day rates of change, sedimentologic implications, and information on the origin and modification of the sand sheet, as well as to provide baseline surficial sedimentologic data for comparison with radar reflectivity. Our investigations of surface modification have concentrated on three questions. (1) Does the sand sheet result from erosion or deposition, and when and at what rates have these occurred? McFadden et al. (1987) have shown that aeolian and pedogenic processes play a major role in desert pavement formation, and suggested that such close-spaced angular fragments originate as surface deposits. In contrast to desert "pavement", the subrounded granule veneer of the sand sheet may be the opposite endmember of the desert surface, originating in the subsurface and exposed by aeolian redistribution and erosion. The origin of the sand sheet by net deflation (Sandford, 1933) or by climatic cycling (Haynes, 1982b) may not be mutually exclusive, however, and estimates of the present rates of erosion from remote sensing and field observations allow a first quantitative estimate of net sediment flux. (2) What are the relationships among the various scales of large ripples measured in the field and brightness patterns (chevrons) detected by orbital data? Breed et al. (1987) provided the first detailed description of giant ripples in this region, which have a wavelength of about 500 m, and are visible on the ground only where dark lag deposits are exposed in inter-ripple "hollows". In the southern part of the Selima Sand Sheet the surface becomes undulatory where giant ripples have amplitudes of up to 10 m and wavelengths up to 1 km (Haynes and Johnson, 1984). However, in our present area of study, the low amplitude, giant ripples grade laterally into even larger scale chevron-shaped bedforms (Maxwell and Haynes, 1989) that for several years eluded an exact demarcation on the ground because of their extremely low amplitude. Whether these features are replenished from local deposits, result from long distance transport, or a combination of sources remains open to question. (3) Finally, the origin of this part of the desert has been ascribed to denudation and cliff retreat. If we extrapolate the processes seen today and interpreted from the Quaternary history, does this help to explain the low relief surface that forms the Selima Sand Sheet?

In addition to these questions of sand sheet origin and sediment transport, the identification of active sand allows us to document the location and characteristics of the mobile component of the sand sheet, which will eventually enable the mapping of near-surface stratigraphy. In the Safsaf oasis area at the eastern margin of the Selima Sand Sheet, Davis et al. (1993) used a Landsat Thematic Mapper image (acquired November, 1984) to map surficial deposits based on reflectance characteristics in the visible and near infrared bands (bands 1, 4, and 7). They found that some of the radar-detected fluvial channels were visible at these wavelengths, which they attributed primarily to subtle compositional variations; either the exposure of more iron-rich material, or its

entrapment by subtle topographic depressions. Based on these results and the rapid changes seen in Landsat images from different years, the identification and mapping of buried topography depends on our ability to delineate active surficial deposits, and to test whether exposed lag deposits are a product of topographic undulations on an old surface.

2. The Selima Sand Sheet

As described above, the surface of the northern Selima Sand Sheet is a monotonous, flat, vegetation-free expanse of sand and granules, broken only by isolated dune fields, nearly imperceptible giant ripples (Breed et al., 1987), and by widely scattered remains of Sudan Defense Force (SDF) and Long Range Desert Group (LRDG) camps (Haynes, 1985). The sand sheet extends from just east of the Gilf Kebir plateau to the Kiseiba Oasis region, a distance of ~ 400 km, and from Bir Tarfawi at the north edge to latitude 21° in northwestern Sudan (~ 300 km). Several barchan fields override the sand sheet in response to the dominant (north) wind, and a few vegetated but unoccupied watering places are located on the east and northeast edges: Bir Shep, Selima, Bir Kiseiba and Bir Tarfawi (Fig. 1). The shallow depression surrounding Bir Tarfawi is the location of several inset lacustrine deposits that range in age from > 500 kyr to 4000 bp (Wendorf et al., 1993; Szabo et al., 1995). Pollen records at Selima Oasis indicate a fluctuating water table, with the latest high stand at 8.7 to < 6 kyr (Ritchie et al., 1985; Haynes et al., 1989). Thus, long-term climatic changes are viewed to be responsible for cycles of deflation, lacustrine deposition, and re-excavation of the scattered oases. It is likely that once the local bedrock is weakened by near-surface groundwater and effluorescence, the oases became sites of preferential erosion. Whether the same process can be applied to the remainder of the sand sheet is more difficult to determine. The extensive surficial limestone and kunkar (fragmented phreatogenic carbonate) deposits

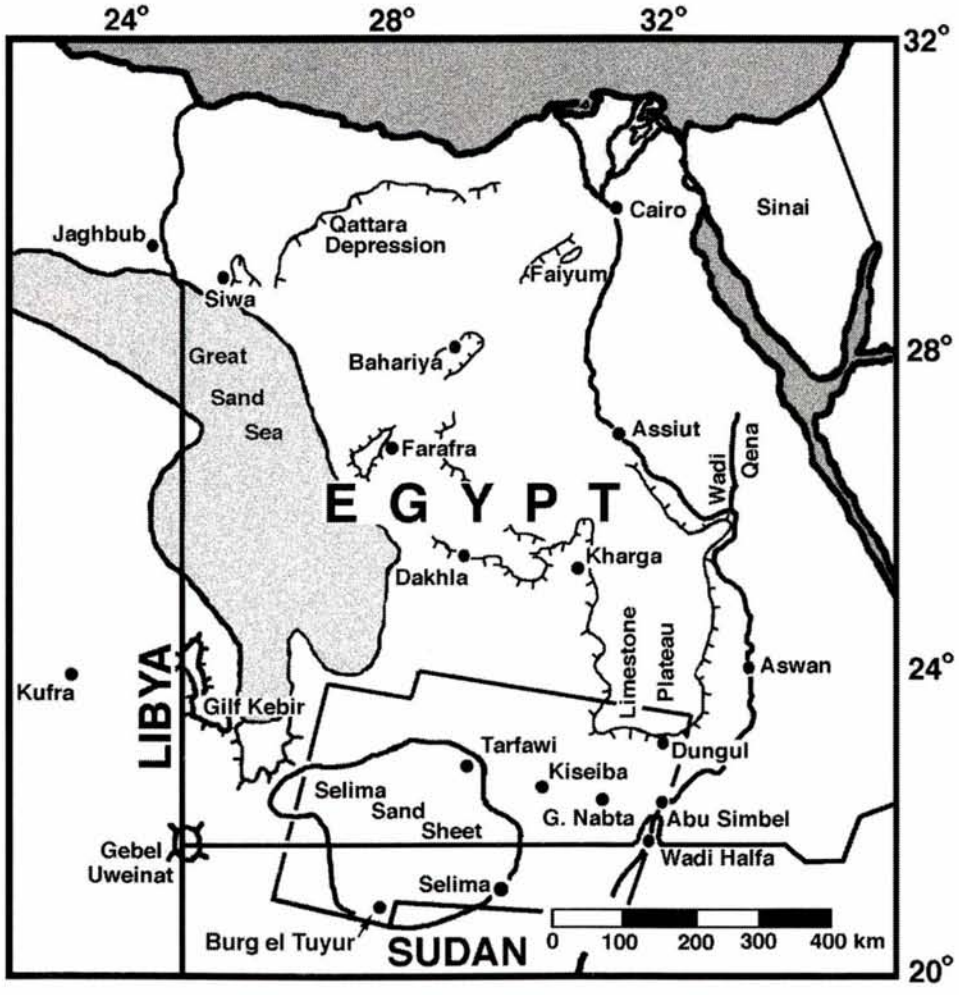

Fig. 1. Location map of Egypt showing area of Selima Sand Sheet at the border of Egypt and Sudan. Outline denotes area of mosaic shown in Fig. 2.

that extend for 20 km west of Bir Tarfawi suggests the presence of an extensive lake or high water table at > 350 kyr, and at ~ 277 kyr, the oldest distinct moist periods determined via Uranium-series dating of sediments from the sand sheet (Szabo et al., 1995). It is possible that a water-table-controlled planation surface (Stokes, 1968) could have been the penultimate control on base level erosion, but evidence for such a surface is lacking. If base level were controlled by a paleo-water table, we would expect a more-or-less planar zonation in sediments beneath the aeolian sand sheet deposits. In addition, despite a thorough search for terrace deposits on the lee side of the hills northwest of Bir Tarfawi, we have found no indicators of the extent of earlier lakes other than the deflation-resistant kunkar that is locally present near Bir Tarfawi.

Sand sheet microstrata are composed of laminated bimodal mixtures of fine to medium quartz sand laminae, usually less than 10 mm thick, separated by single grain thicknesses of subrounded to rounded quartz granules (1.5–2.5 mm diameter) (Maxwell, 1982; Breed et al., 1987), similar to those defined by Folk (1971) for the Simpson Desert of Australia and Warren (1972) for the Tenere Desert of the western Sahara. Individual granules form compact surface lags of one grain thickness. As pointed out by Breed et al. (1987) the Saharan sand sheets differ from sand sheets of North America in having essentially horizontal planar laminations (type "b" laminae of Fryberger et al., 1979) as opposed to low angle laminae in American deserts (type "a" laminae).

Thicknesses of the Selima Sand Sheet vary from 1 cm to several decimeters and rarely exceed 1 m except in a few areas, especially in the region of Burg el Tuyur and Bagnold's Barchan in northwestern Sudan, where the amplitude of undulations reaches heights of up to 10 m (Haynes, 1989b; Haynes et al. 1993). Stratigraphic subdivisions within the sand sheet consist of an upper zone characterized by the bimodal laminations and a lower zone where the bimodality is preserved but the laminar structure has been destroyed by bioturbation and pedogenesis. The upper zone has been further subdivided on the basis of incipient stages of pedogenesis into a stage 0, where vertical test pit walls slough to the angle of repose, stage 1 where vertical walls will stand but will ablate when agitated either by hand or by wind, and stage 2 where a medium prismatic pedogenic structure has developed with peds measuring 2–3 cm diameter and rarely exceeding 10 cm in length. The characteristics of these stages are summarized in Table 1, and this nomenclature is used in the stratigraphic sections presented below.

Active surface sand sheet everywhere in the Arba'in Desert is stage 0, and where associated with stages 1 and 2 they may represent a chronosequence. However stage 0 has in a few cases been observed below stages 1 and 2, and it is not uncommon to find a stage 1 below a stage 2. Therefore stages 0, 1, and 2 do not necessarily represent a chronosequence in areas where they are not sequential. Instead we suspect that these incipient stages 1 and 2 are the result of the very infrequent local rainfall events that occur at intervals of 30–40 yr (Haynes, 1987).

In many areas stage 0, 1, and 2 sand sheets are underlain by older sand sheet deposits that are massive yet retain their bimodal sand sheet texture. The laminar structure has been destroyed by bioturbation during pedogenesis, and cohesion is significantly greater in these stage 3 and 4 paleosols. Test pits excavated in the sand sheet in northwestern Sudan revealed sand sheet with stronger color values, cohesion and prismatic structure than stage 3, which was thus designated stage 4 (Haynes and Johnson, 1984). In both stages, very coarse prismatic peds are separated by sand-filled cracks up to 0.5 cm wide. All stages 3 and 4 paleosols are invariably separated from overlying lesser stages by a sharp erosional unconformity.

In many areas these sand sheet deposits unconformably overlie sand and gravel alluvium with varying degrees of pedogenesis and calcification. In the large buried channels revealed by SIR-A radar images (McCauley et al., 1982) the alluvial deposits are light gray (10YR) to light brownish gray (7.5YR) to white where strongly cemented by calcium carbonate (stages III and IV of Machette, 1985). On the low uplands away from the buried SIR-A channels or depressions, alluvial deposits show varying degrees of induration from firm, friable to hard with colors ranging from browns (7.5YR) to reddish brown (5 YR) to red (2.5YR) and stages of calcification ranging from stage II to stage III. Alluvial units beneath the sand sheet stages are referred to by our field designations, fine pebble alluvium (FPA) and calcified pebble gravel (CPG) with no age distinctions or implied correlation with units farther to the south (Haynes et al., 1993).

The documentation of modern erosion and deposition in the sand sheet is made difficult because of the absence of large bedforms and stratigraphic marker horizons. Sand transport has been quantified only by observations of the infilling of historical remains (Haynes, 1985), and by remote sensing studies of surficial changes (Maxwell and Haynes, 1992). Changes in the surface of the sand sheet were first noted in 1986 when we compared light- and dark-toned areas on a 1972 Landsat image with the present distribution of coarse granule lag and horizontally truncated ripples seen in the field. Since then, we acquired two MSS scenes and two TM repeat scenes to document the apparent movement of dark- and light-toned patterns. Based on field surveying, we identified several scales of extremely long wavelength, low amplitude "ripples", ranging from 130 to over 1200 m in a north–south direction, and occurring 10's of kilometers downwind from topographic breaks such as bedrock scarps or barchan dune fields. From correlation between the location of chevrons in the field and their appearance

on orbital images, we interpreted the light chevrons to be areas of active sand sheet deposits that cover the coarse granule component present in darker areas (Maxwell and Haynes, 1989). Dark, discrete chevrons are most likely the stoss sides, and owe their lower reflectance to an admixture of darker grains eroded from older sand sheet and alluvial deposits with stage 3 or higher paleosols.

Based on our prior work and the preservation of camp remains from early explorers, the surface is not strictly deflationary as envisioned by prior workers. Indeed, the action of wind typically accentuates irregularities in a non-cohesive irregular surface (Peel, 1966), so the development of a sand plain from an initially rough surface is not at all intuitive. Since we cannot resolve past climatic effects from the present surface topography, we need to look at the near-surface stratigraphy as well as present-day activity as a means of determining the net flux and rates over the present hyperarid interval. To do this, we first present the results of investigating the shallow-surface stratigraphy, coupled with remote sensing and field monitoring over the period 1987–1994.

3. Multitemporal observations

We carried out surveys in one of the flattest parts of the sand sheet, an area of prominent chevrons located 140 km west of Bir Tarfawi (location A, Fig. 2), the site of one of the longest records of human habitation in the Darb el-Arba'in Desert (Wendorf et al., 1993). Three methods were used for monitoring modern changes in the surface: multitemporal, co-registered remote sensing data, repeated topographic surveys (each time documenting the near-surface stratigraphy), and deployment of survey pins at locations along the survey lines and where minor variations in the surface were noted. Three N–S survey lines were established in 1987, 1989, and 1992 (Fig. 3), and each of these lines was re-surveyed, two of them more than once. An exact match of resurvey dates and repeat Landsat image dates does not exist because planned field work did not always take place, and planned image acquisition was not always possible. Nonetheless, the data presented here show variations measured over time periods ranging from 1 to 5 yr.

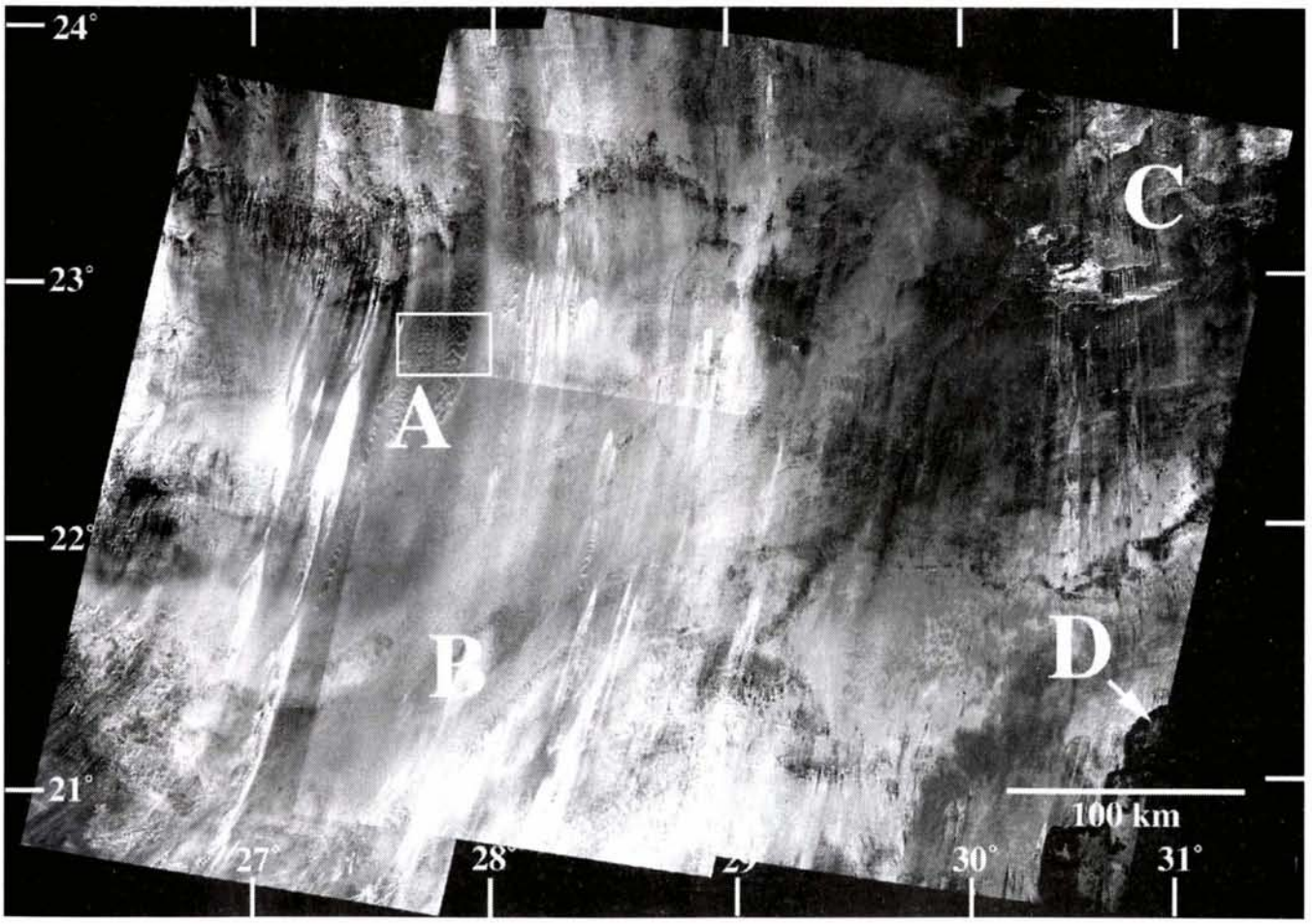

Fig. 2. Mosaic of Landsat images of southern Egypt: (A) area of prominent chevron patterns monitored since 1987; (B) radar-detected channel trending ENE in the sand sheet; an additional less distinct (in near IR) channel is present north of that marked "B"; (C) limestone plateau that separates the northern part of the sand sheet from the Nile Valley; (D) upper end of Lake Nasser. Mosaic is composed of parts of 8 Landsat images obtained between 1973 and 1992. Bright SSW streaks are barchan dune fields.

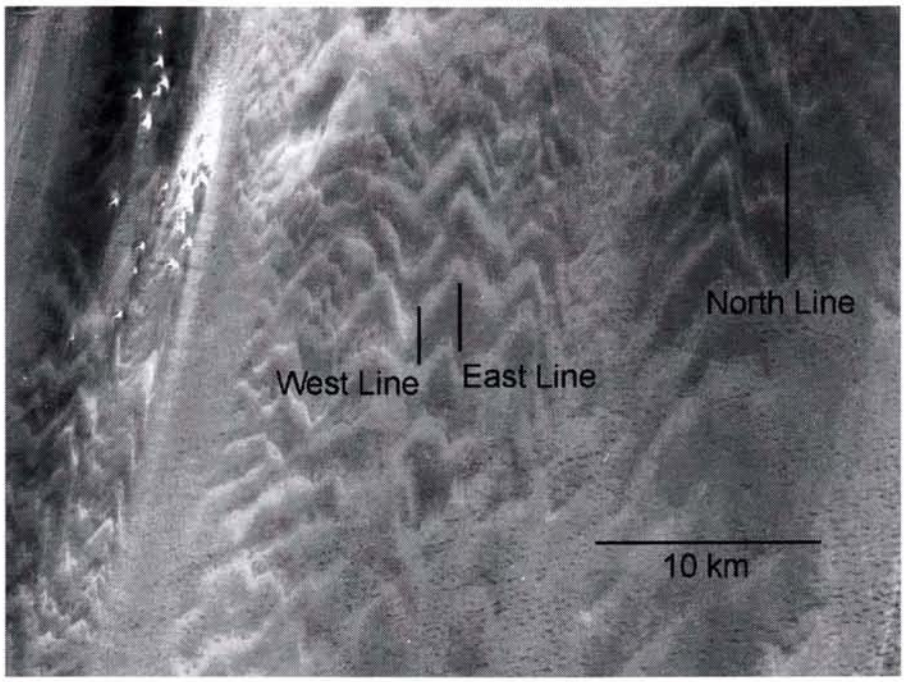

Fig. 3. Location of Field Survey Lines for detailed study of the sand sheet (at location "A" in Fig. 2. Base image is a 1992 Landsat Thematic Mapper scene (Band 7), and geometric correction of scenes from all dates was done on a much wider view to include stable rock outcrops and hills for image registration. Individual barchan dunes at the left side of this scene are ~ 800 m across.

We used Landsat scenes acquired in 1972, 1986, 1988 and 1992 to determine changes in the distribution of light and dark chevron patterns at the surface. Slight variations in surface patterns exist in all spectral bands (of both the MSS and TM sensors), but the delineation of chevrons is greatest in the near-infrared. All scenes were obtained in winter months (October through March), and although several attempts were made for simultaneous field work and orbital acquisitions, the closest we came to simultaneous observations was in 1992 when we were able to obtain a TM scene three weeks after leaving the field. We converted all image data to spectral radiance following procedures outlined in Markham and Barker (1986) to remove variations due to sun elevation, camera gains and offsets, and seasonality. The brightness values thus calculated are essentially exoatmospheric reflectances, and although variation in reflectance between the scene dates can be caused by differences in aerosol composition, we assume that this contribution was constant. Like Davis et al. (1993), we are forced to estimate haze contributions in these scenes because of the absence of true shadows that could be used to apply more conventional algorithms. Markham and Barker (1986) suggested that uncertainties in exoatmospheric reflectance resulting from sensor changes with time are less than 2% for the MSS instruments, near the range in variations of surface reflection that we are studying. However, the discrete spatial patterns of chevron changes allow their discrimination. Registration of the scenes was done using field control points obtained by global positioning system fixes obtained on dunes (whose maximum movement can be estimated at 60 m between 1986 and 1994 (Haynes, 1989)), isolated patches of bedrock, and the dark hills to the north of the study area. Bilinear interpolation was used in resampling, and geometric correction typically resulted in 100 m or less rms error. Reflectance profiles discussed below were obtained by taking 10 pixel (at 30 m resampling for both MSS and TM data) averages in an east–west direction across the survey lines. Although this results in some "smearing" of the data, it overcompensates for the geometric error in registration.

Repeated field surveys were done with a laser electronic distance measurement theodolite (EDM) with an internal distance accuracy of ~ 1–2 mm. In practice, we found that the accuracy of repeated elevation measurements was on the order of 1–2 cm (in different years and over several hundred meters of baseline), which we attribute to the unavoidable problems of using different instruments, and international and field transport handling as well as operator error. In 1992, in particular, we noted a systematic error with elevation values that we later found resulted from an internal instrument leveling misadjustment. Surveying of more "normal" topography would never have detected such a minor discrepancy, but in this area (where we have found it necessary to subtract earth curvature from our plots), such relatively minor adjustments limit our ability to measure changes in sediment thickness. In order to compare the multiyear plots

presented below, we reduced all profiles by deriving a best-fit linear curve to each year's data, and re-projected each survey line with a slope of zero and an intercept based on minimizing the variance between the line and the surface elevations indicated by the survey pins. With the exception of the instrument error noted in 1992, these corrections typically resulted in a 1–4 cm shift in elevation values over survey lines of several kilometers. Additional sources of error are noted with the individual survey lines described below.

The most accurate method utilized for determining temporal changes in surficial erosion and deposition is through the repeated measurements of the exposure of survey pins left along the lines since 1987. All pins (except the 0 point on the East Line) were left with the top 14.5 cm above ground level, and the elevation was measured each subsequent year of field work. The vertical changes of 1–2 cm of both erosion and deposition attest to the activity of the sand sheet, and are for the most part consistent with observations from orbital data.

Repeated delineation of the sand sheet stratigraphy is more subject to "operator" error than any of the other monitoring techniques. Both authors classified and measured the thicknesses of sand sheet stages during each field season, and although we "calibrated" each other on several occasions, we still found discrepancies in classification of the less pedogenically altered units (stages 1 and 2) because of their transitional nature. For this reason and the observations of the stage 0 changes indicated by the survey pin data, we rely on the stage 2/3 and stage 0/1 contacts in determining stratigraphic markers between older sand sheet deposits and more recent changes, respectively. Below, we summarize our sand sheet surveys combining remotely sensed data and field observations.

3.1. East Survey Line

The East Survey Line is located 11 km due east of our camp dune, and was chosen to cross a prominent bright chevron visible in a 1972 Landsat scene. Hand-dug pits to ~ 30 cm were spaced at 10 m along the northern part of the line when first surveyed in 1987, and at 20 m spacing on the southern half of the line in 1988 for a total distance of 2.8 km (Fig. 4). It was here that we initially noted a systematic variation in sand sheet stage with topography. In places, the active sand sheet (stage 0) directly overlies a stage 4 deposit, and typically at "higher" elevations, the younger stages (0–2) are superposed on older deposits (Fig. 5).

Variations in the surface reflectivity of the East Survey Line between 1972 and 1992 are shown in Fig. 6. Although we had located the line based on a 1972 Landsat scene, it is evident that by the time of our first surveys in 1987 and 1988, the surface reflectance had changed. The 2-yr period between the Landsat scene dates of 1986 and 1988 straddles the timing of our initial surveys, and a bright chevron that was located just north of the line had migrated to the central part of the East Line by 1988 at a net rate of ~ 600 m/yr. In doing so, the pattern also shifted slightly to the west, so that at the times of our surveys, we were then located on an oblique portion of the light chevron (Fig. 6). By 1992, the time of our re-survey of the northern part of the line, the pattern had again changed, with the entire survey line located on a broad band of intermediate-toned material downwind of a prominent bright chevron (Fig. 7).

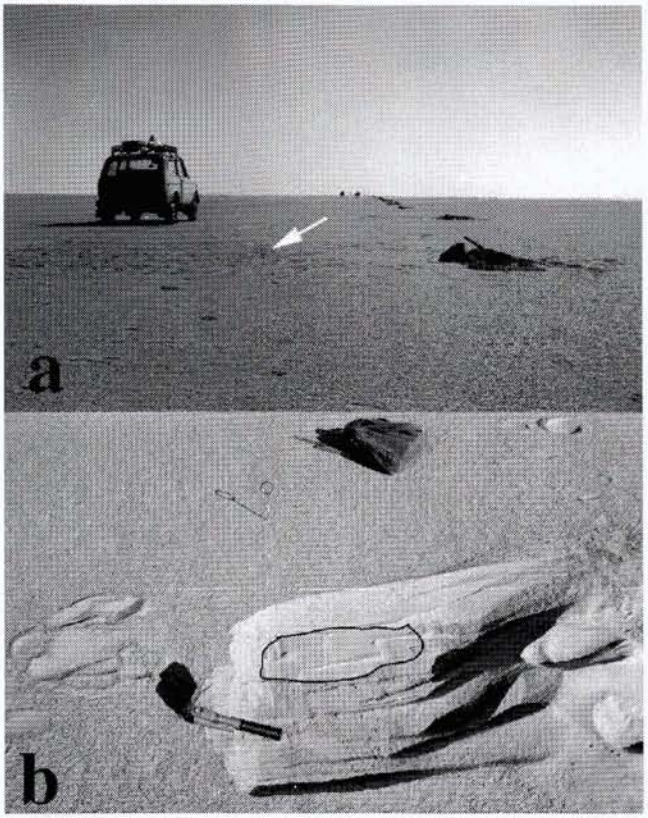

Fig. 4. (A) Field view of East Survey Line looking to the south. Survey stake between jeep and pit is one of those used for repeat monitoring of erosion and deposition at the surface. (B) View of pit 50 on the East Survey Line 1 yr after initial survey (the pit is the fine sand, semicircular pattern at the top of the scraped area). No surface trace of the original pits is visible from year to year, although the spoil piles are visible by a greater concentration of coarse pebbles dug from gravel alluvium at the base of the pits.

These reflectance changes along the survey line are shown graphically in Fig. 8. The 1972 reflectance data on this and subsequent plots are shown to give an indication of the magnitude of change over the 20 + year period, but the patterns can only be traced on a shorter time interval. Comparison of the 1986 reflectance values (averaged over a 300 m section perpendicular to the line) with the image shown in Fig. 6 indicate that the bright areas at the north and south ends of the survey line are ~ 3% brighter than the dark patch at the center of the line (just

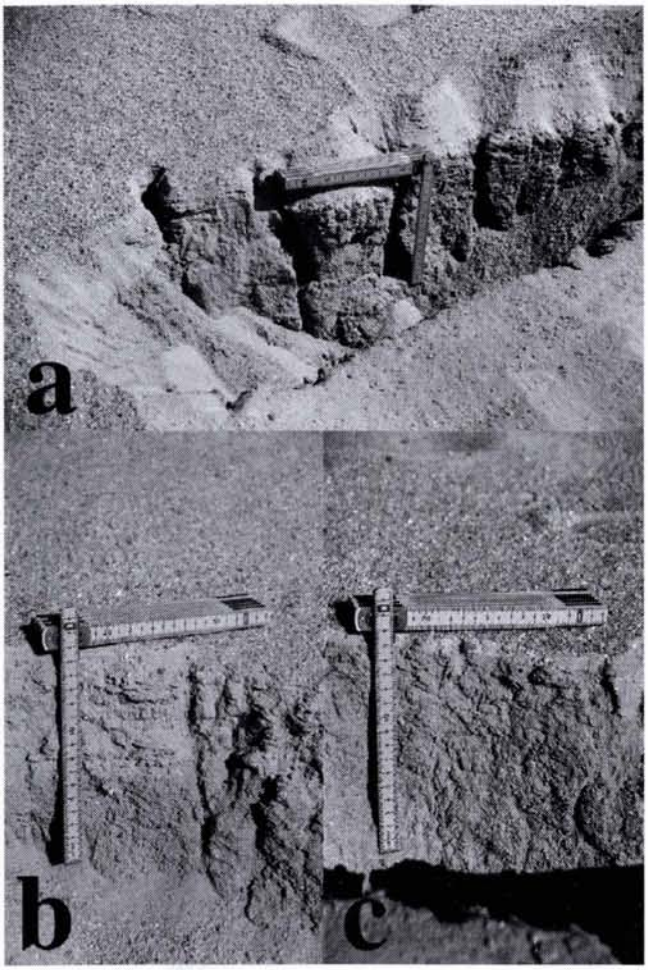

Fig. 5. Selected photos of pits in the East Survey Line showing variation of sand sheet stages and associations: (A) shallow trench at pit 11 showing range in stage 0 thickness (3–4 cm near ruler to 5–6 cm thick to the right) overlying stage 4 sand sheet with prominent cracking pattern. (B) 1–2 cm stage 0 overlying 8 cm stage 2, overlying stage 3 sand sheet at pit 35. (C) monolayer of active sand sheet (stage 0) overlying truncated stage 3–4 sand sheet.

south of the 0-point noted in the plot and on Fig. 6). In 1988, the bright ends remained constant, but the central part of the line became brighter, and by 1992, there was little structure along the line, only a slight monotonic decrease in reflectance from north to south.

Unfortunately, we had put only one survey pin in during the initial survey in 1987 (at location 0, Fig. 8). When we re-measured the pin in 1988, 0.5 cm of erosion had occurred at that location. Most of the changes in the surface elevation along this survey line took place between 1988 and 1992. During that 4-yr period, location 0 had 0.5 cm of deposition, while the south-central part of the line was eroded by 1 cm, and the southernmost point had 2 cm of sand sheet deposited. The net deflation at 450 and 900 m is consistent with passage of a light thin sand deposit between 1988 and 1992, but the deposition of 2 cm at the south end of the line during the same period that a light chevron had migrated south of the survey line is opposite the expected outcome if the darkening resulted from erosion of the active sand sheet. However, as can be seen in the 1992 TM image (Fig. 6), the south end of the line was still in a zone of intermediate reflectance in 1992, with the darkest reflectance at the midpoint of the southern half of the line (900 m), consistent with a hypothesis of erosional darkening, since there was ~ 1 cm of net erosion at that location between 1988 and 1992. With the exception of location 0, the entire East Line shows a gain of a few millimeters between 1992 and 1994, indicative of the light chevron that was poised to migrate through the region in 1992. We were unable to obtain a corresponding image in 1994 to test this because of cloud cover that persistently obscured the region on every acquisition date until well into the sandstorm season (mid-March).

The initial survey of the northern part of the East Line led us to suspect that there was much more topographic variation of the sand sheet than meets the eye (Fig. 4). Both the "large" undulations at ~ -500 m and smaller undulations indicated that the surface had extremely long wavelength chevrons (Maxwell and Haynes, 1989). To test whether it was these ~ 10 cm high features that were causing the major reflectance variations, we resurveyed the southern part of this line in 1989 (a 1-yr interval), and the northern part in 1992 (a 5-yr interval). The plot of topography in Fig. 8 indicates that both the large- and small-scale undulations are stable over both of these periods, and in fact, the discrepancies between the topographic profiles at different years are more due to instrument and observer error (the latter responsible for the offset at -600 to -1000 m) than to natural changes. Based on the repeated monitoring of survey pin exposure, it is apparent that net yearly changes are on the order of a few mm's; we therefore trust only portions of our topographic surveys for monitoring purposes, where elevation variations are indicated along the same instrument set-up, or where we have control by survey pins. The gross (> 1 cm) topography revealed by the surveys holds up under multiple observations, however, and also makes sense when combined with the near-surface stratigraphy.

Not all of the sand sheet stages (Table 1) are present in each section; most commonly, stage 0 is present in thicknesses from a monolayer to a few cms, which may overlie stages 1–4, or some combination thereof. Stage 3 is nearly always present along the East Line, and forms a marker horizon in this region and in many other areas in the Selima Sand Sheet. As shown in the stratigraphic plot of Fig. 8, stage 3 ranges from 1–2 to 30 cm in thickness, and is overlain only sporadically by stages 1 and 2 deposits, typically where there is a shallow trough in the stage 3 upper contact. Stages 0 and 1 are commonly thickest at the crest and in the lee (south) side of the most prominent topographic ripples (locations -600, -450, 300, and

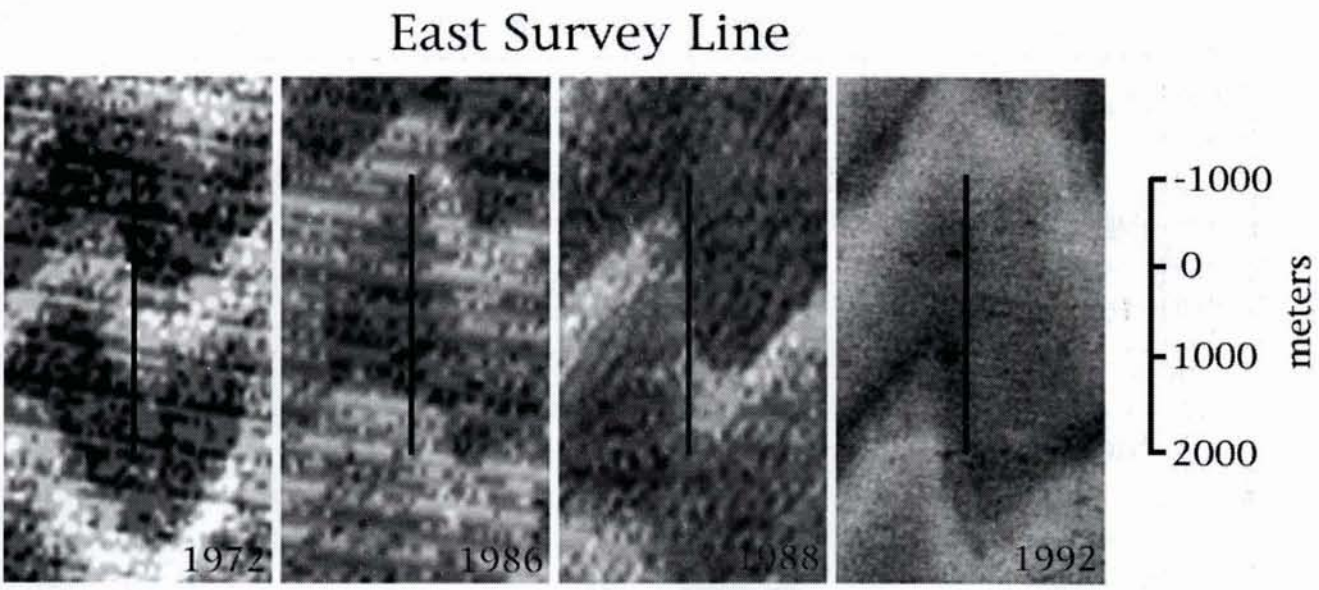

Fig. 6. Near infrared orbital images of the East Survey Line in the sand sheet. 0-point on line delineates northern part of survey (first done in 1987) from southern part (completed in 1988). The 1972 through 1988 subsets are Landsat MSS scenes (Band 4), and the 1992 scene is a Landsat TM subset (also near IR, Band 4). Migration of bright chevrons is best illustrated by comparing the 1986 and 1988 scenes, in which the pattern at the north end of the line in 1986 had moved to the 0-point (and south of there) by 1988.

1500 m in Fig. 8). Both the stages 3 and 4 sand sheet and the calcified pebble gravel (CPG) mimic the present-day topography; CPG is observed primarily at high areas along the line, and appears at greater depths where detected in low areas of the line.

An example of a short-term (1-yr) change in near-surface stratigraphy is shown in Fig. 9. On the lee side of the ripple crest, a greater expanse of stage 1 was present in 1989 than was noted in the field survey from the prior year. Inspection of the Landsat image acquired in 1988 indicates that a bright chevron (stage 0) was present at this location, and most likely migrated to the south by 1989. Although we do not have a 1989 image to confirm this, based on the rapid rate of movement and the change in surface exposure, we believe that the surface change to a stage 1 was accompanied by a darkening of the surface due to exposure of the older unit as the stage 0 chevron moved off. Elsewhere along the East Line, the primary changes noted from re-surveying were variations normally less than 1 cm in the thickness of the active stage 0 sand sheet.

3.2. *West Survey Line*

The West Survey Line, a 2.5 km transect located 2 km west of the East Line, was established in 1989 to test the lateral (east–west) variability of sand sheet stratigraphy, and to further check our monitoring of surficial changes in a longitudinal direction. As shown in Fig. 10, changes in reflectance patterns here also indicate movement of light chevrons, most visible between 1986 and 1988, at a net rate of $\sim$ 500 m/yr. Some of the high frequency variations in 1986 are due to the residual striping in the MSS scene, but the overall $\sim$ 2% brightening of the area between 500 and 1500 m is apparent in both image and graphical format (Fig. 11). In both 1988 and 1992, the northern half of the line is dominated by a bright chevron. Prominent changes in reflectance patterns are present east of the line and are particularly distinct in the TM image acquired in 1992 (Fig. 10).

With the exception of the northernmost point on the line, the variation in erosion and sedimentation represented by the survey pins is all within a 1.5 cm envelope. Three pins at the south end of the line suggest about a centimeter of deposition between 1989 and 1992, and minor erosion between 1992 and 1994 (Fig. 11). At 1000 m, the location of the bright chevron in 1988 and 1992, no net change was detected between 1989 and 1992, although we suspect that the surface materials responsible for the bright chevron seen in 1992 may not be the same as those in 1989 because of the rapid motion of these thin bedforms. In contrast to these minor changes, the north end of the line experienced 2 cm net erosion between 1989 and 1992, and another 0.5 cm of downcutting took place in the next 2 yr. This location was in a dark zone depicted in the image data at those same time periods, and it was likely in a similar dark chevron at the time of the final field measurement in 1994.

Topographic changes between the surveys over the 1989–1994 time period show more variation, apparently due to instrument and operator inconsistencies rather than to real surface changes. Both sets of data track well in the first 900 m of the line, but beyond that, major trends of highs and lows remain, but their magnitude is

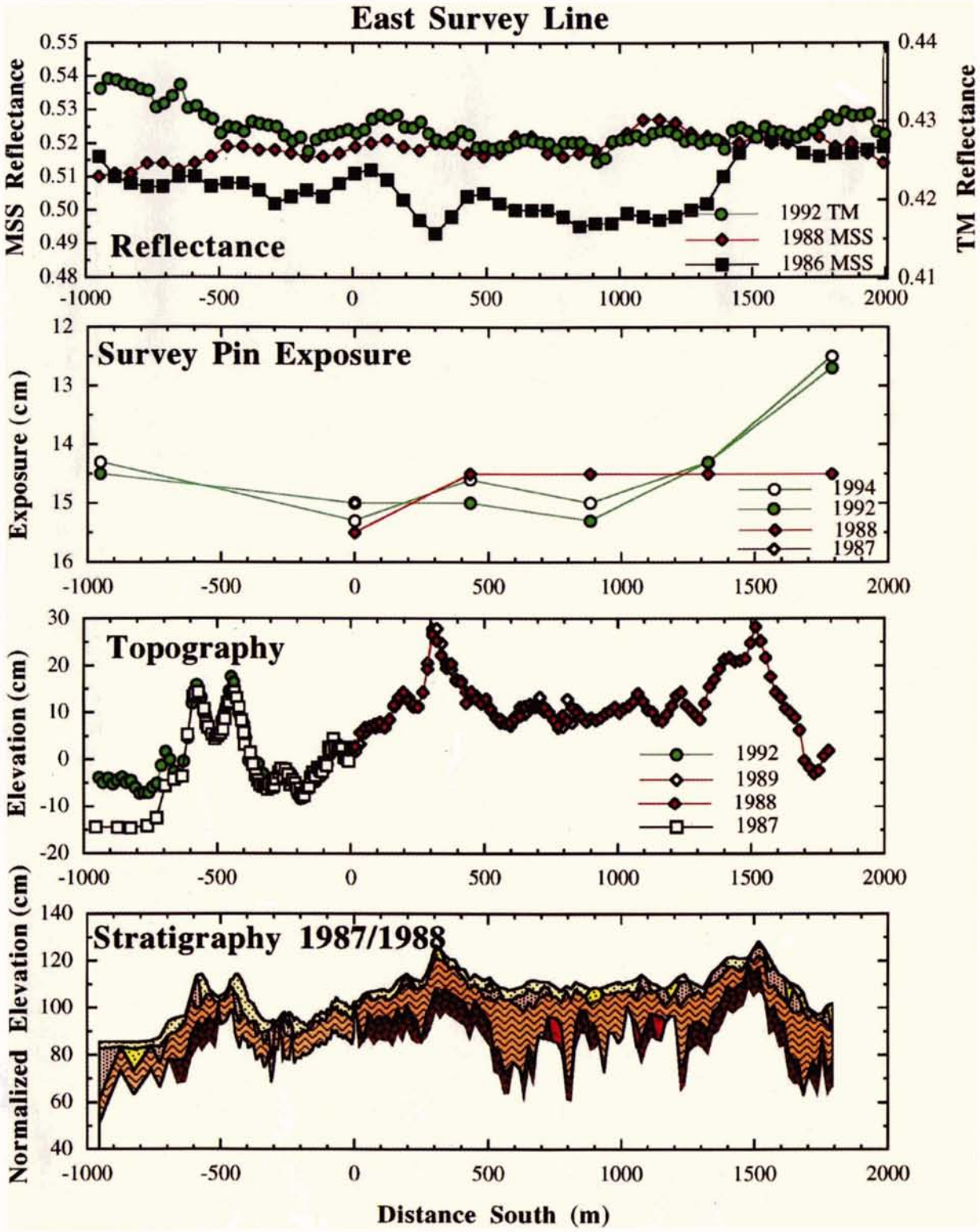

Fig. 7. Summary of observations along the East Survey Line. Reflectance values are derived from the averages of 300 m wide swaths along the line after radiometrically correcting the images. The differences between MSS and TM reflectance scales are due to the different bandwidths of each camera. Survey pin exposure indicates the amount of erosion and deposition adjacent to survey pins; vertical scale is the distance from the top of the pin to the sand surface, and is shown in reverse order to graphically depict erosion and deposition. Topography represents the relative elevation of the sand sheet after correcting for instrument variation and minimizing error (see text). Vertical exaggeration = 1640x. Stratigraphy is derived from hand-dug pits at 10–20 m intervals along the line, and is shown at less exaggeration than topography plot above. Legend for stratigraphy is shown in Fig. 8.

Table 1
Characteristics of sand sheet units

Stage	Stratification	Texture	Thickness
0	Well-developed planar horizontal; does not hold vertical face when excavated	Bimodal fine sand and granules	Commonly one lamination thick, but may be up to 10's of cm in aggradational zones
1	Well-developed planar horizontal; retains vertical face when excavated	Bimodal fine sand and granules	2—4 cm common, up to 10—20 cm
2	Well-developed planar horizontal stratification interrupted by medium prismatic structure	Bimodal fine sand and granules	0—10's of cm
3	Weak, coarse prismatic structure (cracking pattern) with little evidence of horizontal stratification	Primarily bimodal fine sand and granules with addition of clays and minor carbonates	0—20 cm
4	No evident stratification; well-developed coarse prismatic structure (cracking pattern)	Primarily fine sand and granules with clay component and local fine pebble alluvium	0 – > 30 cm
Fine pebble alluvium (FPA)	No stratification; may have cracking pattern depending on texture	Generally sub-angular to sub-rounded pebbles with admixture of clays in fine component	0– > 30 cm
Calcified pebble–gravel CPG)	No stratification or cracking pattern	Coarse-grained polymict alluvium /colluvium	5 cm + ; usually the basal part of the hand dug pits; in areas outside the sand sheet, may grade into $CaCO_3$ kunkar

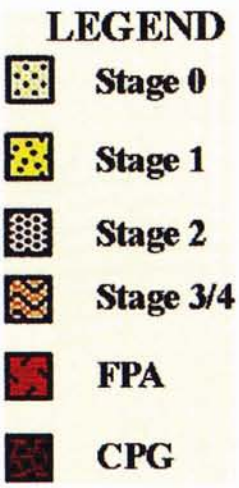

Fig. 8. Legend for sand sheet stages of pedogenesis, fine pebble alluvium (FPA) and calcified pebble gravel (CPG) used in subsequent figures.

much more variable. For that reason, we do not trust the temporal variations in measured topography from the 1994 re-survey. However, the topographic data do provide a baseline for depicting stratigraphic variations. Similar to relations in the East Line, stages 0 and 1 reach their greatest thicknesses in the lee of the most prominent ripples (at 1000, 1500 m and south of 2000 m, Fig. 11). Stage 2 sediments both infill local lows in the stage 3/4 upper surface, and form prominent highs in the southern half of the line. At those locations, stages 0 and 1 are only a single lamination, if present. Finally, superimposed on the short wavelength (~ 100 m) highs and lows of the stage 3/4 surface is a broader, 500–800 m undulatory surface that mimics long wavelength variations at the top of the sand sheet.

Comparison of the stratigraphy and topography between the East and West Lines indicates that there is no lateral continuity between the two lines despite their parallel setting in the unimodal wind regime. Instead, the rippled planform of the surface as depicted in the Landsat images is consistent with each line having its own high and low points; even the long wavelength ripples in the stage 3/4 surface of the West Line are not traceable laterally to those of the East Line. The minor erosion and deposition documented by the survey pin measurements confirm the longitudinal variations in surface activity, but the interpretation of these changes depends on our hypothesis of rapid movement of the bright chevrons because of the mismatch between the dates of the orbital images and field surveys. By 1989, the time of survey pin emplacement, the bright chevron at the ~ 1000 m mark in the 1988 image had likely migrated to 1500 m, and at a nominal rate of 500 m/yr, this same chevron should have migrated to a point at 3000 m in 1992, south of the survey line. We thus believe that the bright chevron south of the line in the 1992 image (Fig. 10) is the same surficial unit that was present at the 1000 m mark in 1988. The decreased exposure of the survey pins at the south end of the line resulted from deposition of an active sand sheet as the bright chevron migrated past, later to be eroded (as evidenced by the 1994 survey pin measurements).

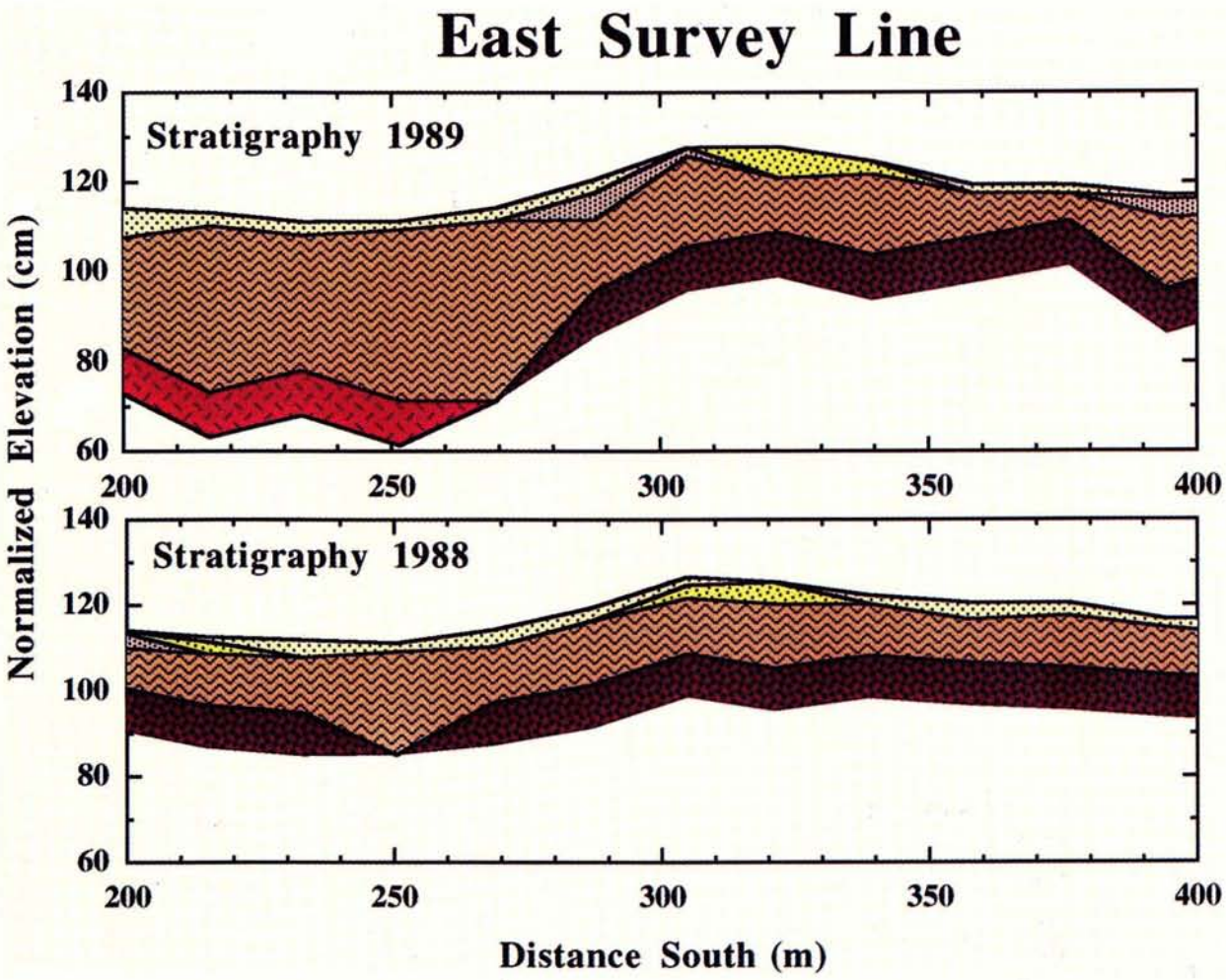

Fig. 9. Detail of repeat topographic and stratigraphic surveys of the East Line centered at 300 m. Between 1988 and 1989 a bright chevron passed through this area (1988 image is shown in Fig. 6), and the surface showed a less extensive exposure of stage 0 sand sheet on the south side of the ripple in 1988 than in 1989. This scale more accurately depicts the topography of the deposits, but even here, vertical exaggeration is 67x.

3.3. North Survey Line

Based on our experience in comparing the East and West Lines with remotely sensed data, we changed the scale of our topographic and stratigraphic surveys for the North Line, first measured in 1992. Along this 6-km transect, the pit and EDM spacing was increased to 100 m. Fig. 12 shows orbital views of this area in 1972, 1986, 1988 and 1992. Because of both the longer baseline and the more coherent chevron patterns in this area, the migration of these features is easier to see. In 1986, a $\sim$ 1 km wide bright chevron was located at the 3000 m mark, while both the northern and southern parts of the line were in zones of relatively dark sand sheet. 2 yr later, the bright chevron had migrated to $\sim$ 5000 m, and another bright chevron had migrated to the north end of the line (Fig. 12). This rate of movement (1000 m/yr) is twice that observed in our earlier studies and in the other survey lines, but is obvious from the repetition of the patterns in the 1986/1988 data sets. Between 1988 and 1992, the movement of the bright chevrons is more difficult to delineate. Migration of the northern chevron from 500 to 2500 m suggests a rate of 500 m/yr, accompanied by north-south broadening of the feature and more distinct mega-ripple patterns in the dark zones.

Shown in Fig. 13 are only 2 yr of repeat measurements of survey pins along the North Line, both of which were after the latest Landsat acquisition in 1992. Between 1992 and 1994, the area where a bright chevron had been ($\sim$ 2000 to $\sim$ 3000 m) was eroded 0.5 cm, while during the same period, 0.5–1.0 cm of sand was deposited at the south end of the line (5000–6000 m). These changes suggest migration of bright chevron material that was much thinner than that measured on the East or West Lines, which may account for the rapid migration rate observed between 1986 and 1988.

The repeat topographic surveys of 1992 and 1994 do not always show consistent locations of major highs and lows along the survey line, although the amplitude of changes ($-$ 10 to $+$ 20 cm) is the same. After fieldwork

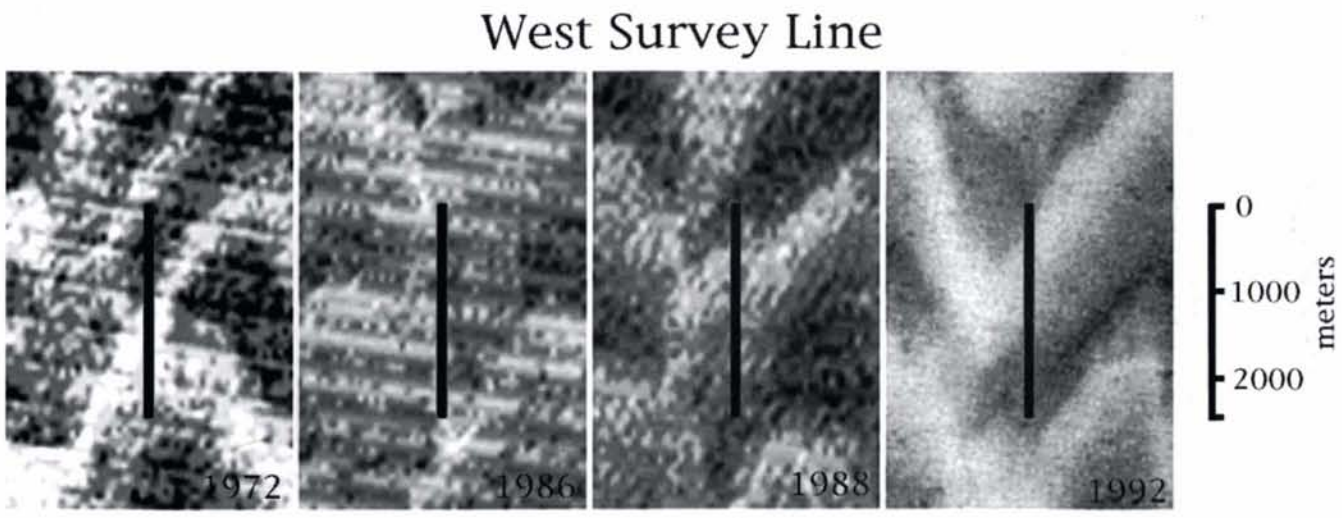

Fig. 10. Near-infrared orbital images of the West Survey Line using same base images described in Fig. 6. Migration of bright chevron from north of the line to the ~800 m area took place between 1986 and 1988, and in the next 4 yr, that particular chevron migrated to a point south of the line. Comparison of the 1972, 1988 and 1992 images indicates that bright chevrons tend to occur at the same position (e.g. the NW trending bright chevron at the ~800 m point), suggesting that they may re-occupy locations controlled by the gentle topography.

in 1992, we discovered an internal leveling error in the EDM, which makes the long-baseline survey in that year suspect. The 1992 survey is shown in Fig. 13 only to indicate the range in elevations over the 6-km line, but we have used the 1994 survey to show stratigraphic variations. In addition to the local topographic "highs" created by 5–10 cm thick stage 2 deposits, broader undulations with wavelengths of 500–1000 m are present in the upper contact of the stage 3/4 material. Also on the North Line, CPG is nearly ubiquitous throughout the line, whereas FPA is only prominent in the major undulations at 1600 and 5200 m. Similar to the stratigraphy of the West Line, a greater thickness of stages 0 and 1 are present on the lee sides of ripples than on the north-facing slopes (e.g. at 1800, 4600 and 5400 m). At the south end of the line, where our survey pins indicated deposition of a minor amount of sand sheet, a review of the stratigraphic measurements does not reveal any increased thickness of stage 0 or 1 sediments, suggesting that this minor amount of deposition (< 1 cm) is not within the resolution of our field stratigraphic measurements.

3.4. Historical evidence for sand sheet dynamics

A longer record of changes in the sand sheet is evidenced by the camp remains of early explorers of southwestern Egypt, those of the LRDG, and widely scattered sites of the SDF. Haynes (1989) reported a constant migration rate of 7.5 m/yr for a barchan that formed the wind shelter for the Ralph Bagnold party on the night of November 2, 1930. The central camp site seemed to be in the same condition as it was left, with one vertical benzene (gas) tin and neighboring food tins inset in the sand sheet. Some of the larger benzene tins had been blown southward. The dune had migrated over the camp, leaving them exposed after it had moved ~400 m to the south. Inspection of the degree of induration of the sand sheet surrounding the tins revealed that they were inset into a stage 1 sand sheet in an area where only a monolayer of sand sheet (stage 0) appears to be active. No paper labels remained and spots of rust occurred on the undersides. Although some of the tins had no doubt been stepped on by members of the original expedition, the number of tins with similar relations found in other camp sites from the 1940s suggests that most tins had been left at or near the surface, and have seldom moved since then. Most WWII-era tins have the original paper labels and pristine, shiny surfaces where buried, further indicative of the hyperarid environment.

Similar relations between sand sheet units and human artifacts were found in the remains of a LRDG camp we discovered on February 8, 1989. This large scatter of wooden box remains, food and benzene tins, and various bottles retained the original camp arrangement despite redistribution of smaller materials by the wind. The tents, cooking fire and most food cans were at the north end of the site, while the motor pool was on the southwest end of camp. In the fireplace, in addition to several bottles, was a copy of the *Johannesburg Times* from July 26, 1942. Like Bagnold's camp from 12 yr earlier, the cans and box remains were set into stages 0 and 1 sand sheet units, and some of the tins were resting on the stages 1–2 contact (Fig. 14). Based on these observations, it is apparent that a stage 0 sand sheet can become a stage 1 rapidly, within a time span of 10's of years. The pristine buried surface of the food tins suggests no extensive involvement of moisture. Instead, the induration likely originates from a brief

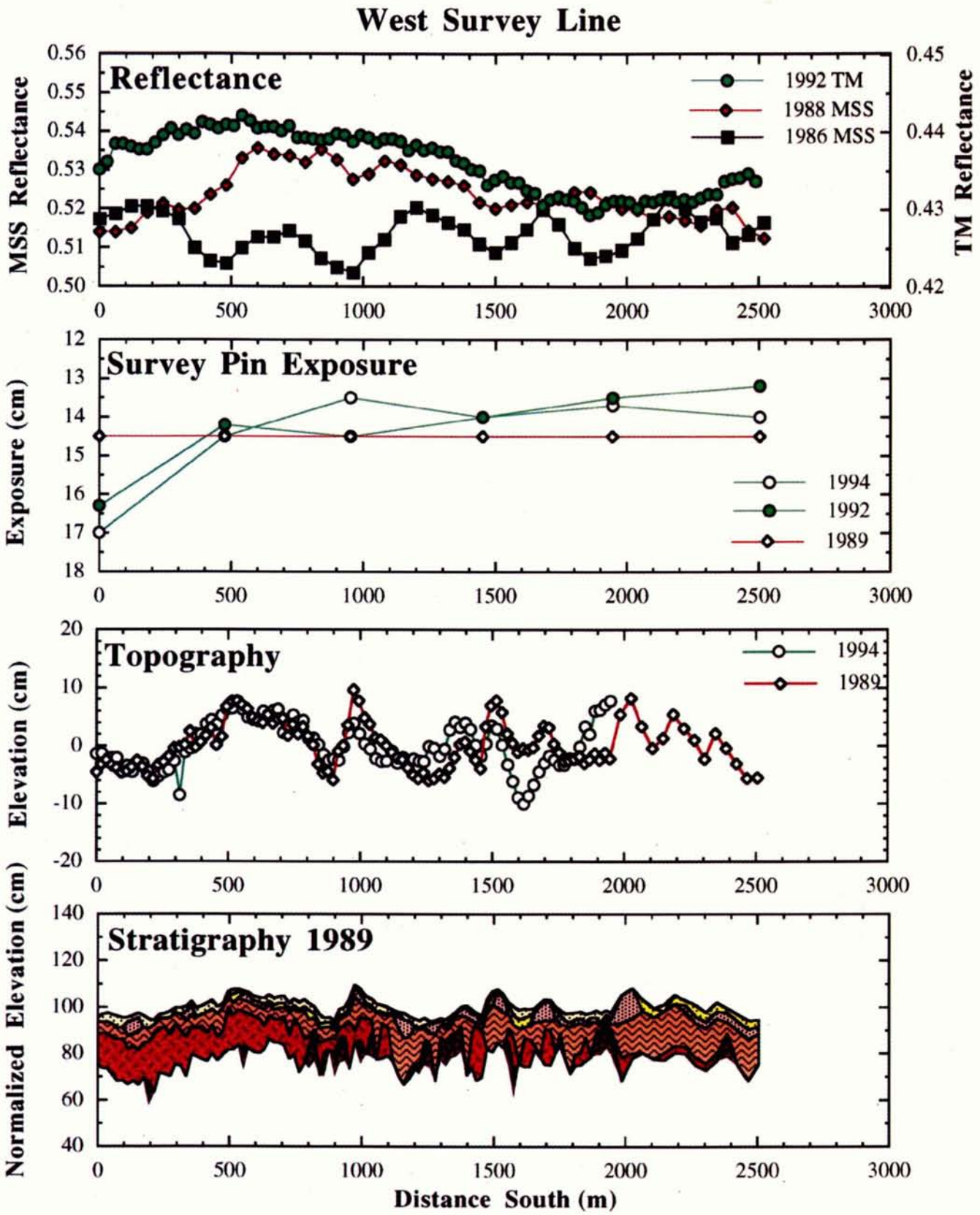

Fig. 11. Summary of observations along the West Survey Line. Near IR reflectance profile in 1992 shows less noise than MSS scenes from 1986 or 1988. Darkening at the south end of the line took place between 1988 and 1992. Deposition of sand also at the south end of the line took place between 1989 and 1992, but minor erosion followed between 1992 and 1994. The stratigraphy measured in 1989 indicates an undulatory surface of both the stage 3/4 and stage 2 surfaces.

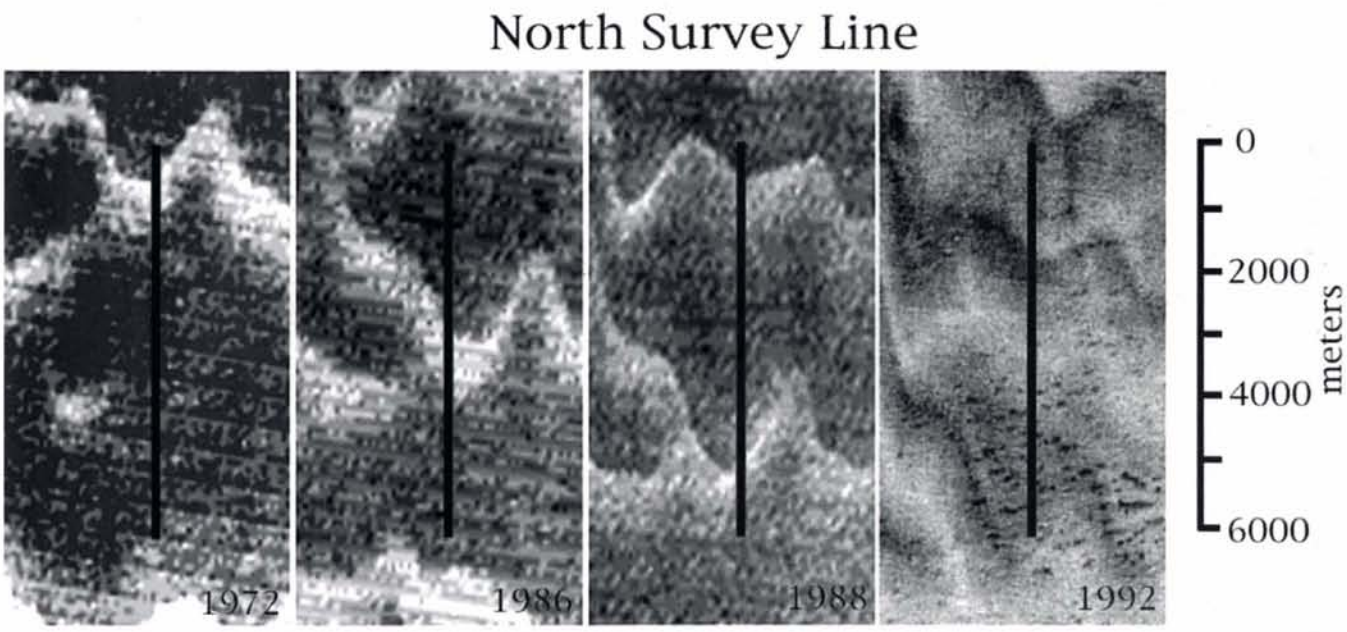

Fig. 12. Near IR views of the North Survey Line. This 6-km line was established in 1992 at a longer pit and survey spacing (100 m) than the West or East Lines for comparison with orbital data.

wetting and an admixture of aeolian transported dust (clays) that allow the original horizontal lamination to stand up to shallow trenching.

To determine the time needed for formation of more highly indurated units of the sand sheet, we use more traditional archaeological indicators. A few kilometers east of the North Survey Line, the remains of a camel (not unusual) were found associated with a few large (20 cm) rocks (unusual). A shallow excavation beneath the rocks revealed a hearth with charcoal that had an AMS ^{14}C age of 825 ± 45 bp (calibrated age of 1235 AD; AA-11500). The hearth is inset under 3 cm of stage 1 sand sheet and overlies another 1–3 cm of stage 1 before grading into a stage 3 (Fig. 14). Consistent with the record of lake deposits from uninhabited oases in northwestern Sudan (Haynes et al., 1979) and tritium analyses on present oasis water (Haynes and Haas, 1980) indicating that the last major period of precipitation was during the middle Holocene, the sedimentation record here indicates that moist conditions which potentially could modify a stage 1 to a stage 2 sand sheet have not been present throughout the past ~ 800 yr. Potentially this site can be used to date the sedimentation rate but as noted by Stokes et al. (1998) in results of optically stimulated luminescence (OSL) dating of the sand sheet, only net accretion can be estimated. No clear age/sediment thickness relations have yet been detected in these measurements, and the net aggradation values have a wide range from 1 to 12 cm/kyr (Stokes et al., 1998).

Two factors that compound the uncertainty in the interpretation of sand sheet aggradation and degradation derived from the hearth's ^{14}C age are the "old wood" problem, and no knowledge of the maximum thickness that may once have covered the hearth. The "old wood" problem stems from the fact that the few sources of firewood in the region today are the dead remains of acacia trees found at vegetated phreatophytic mounds at the remote watering places. Whereas this dead wood has yet to be dated, some could be quite ancient. The other problem is that some sand sheet may have been removed by deflation. There are many examples of resistant items being exposed and truncated by deflation in some areas, such as humans, pottery, and ostrich egg water containers.

The oldest record of sand sheet accumulation comes from Paleolithic and Neolithic archaeological implements found on the surface and in the sand sheet. In one of the pits at the south end of the North Survey Line, we found an accumulation of Neolithic artifacts (from the early to middle Holocene pluvial) inset in stage 3 sediments. Accumulations of stone implements are also found on the north (stoss) sides of the giant ripples, typically where the surficial deposits consist of a monolayer of stage 0 overlying stage 3 or older sediments (Haynes, 1989). However, archaeological remains are notably absent on the lee sides of the same ripples, where stage 2 (and younger) sand sheets may reach thicknesses greater than 1 m. Based on these observations, we believe that the bioturbation and other pedogenic alteration of sand sheet sediments during the Neolithic pluvial were responsible for the transition from stages 1 and 2 to more advanced stages in this area. Elsewhere we have found evidence that modification of sand sheet sediments has resulted from local, presumably

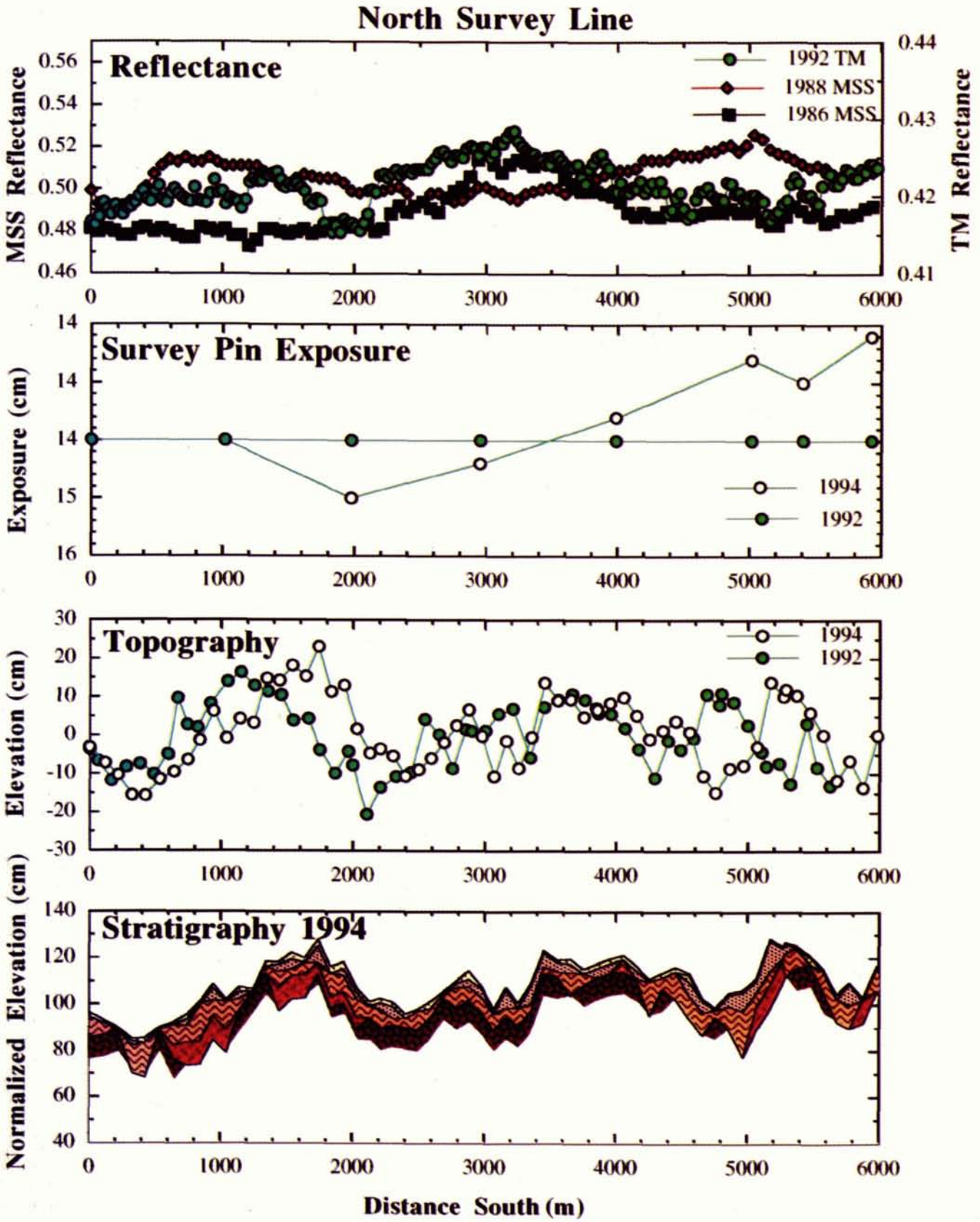

Fig. 13. Summary of observations along the North Survey Line. Reflectance profile indicates a reversal of light and dark zones between 1988 and 1992. In 1992, the bright zone at 3000 m occupied the same position as the bright zone in 1986. Survey pin exposure indicates deposition at the south end of the line between 1992 and 1994, and the re-survey of topographic profiles suggest similar amplitudes of ripples, with the apparent translation most likely due to operator error. Like the other survey lines, the tops of the stage 3/4 and stage 2 sand sheets exhibit an undulatory nature, suggesting early involvement of ripples in producing the present surface.

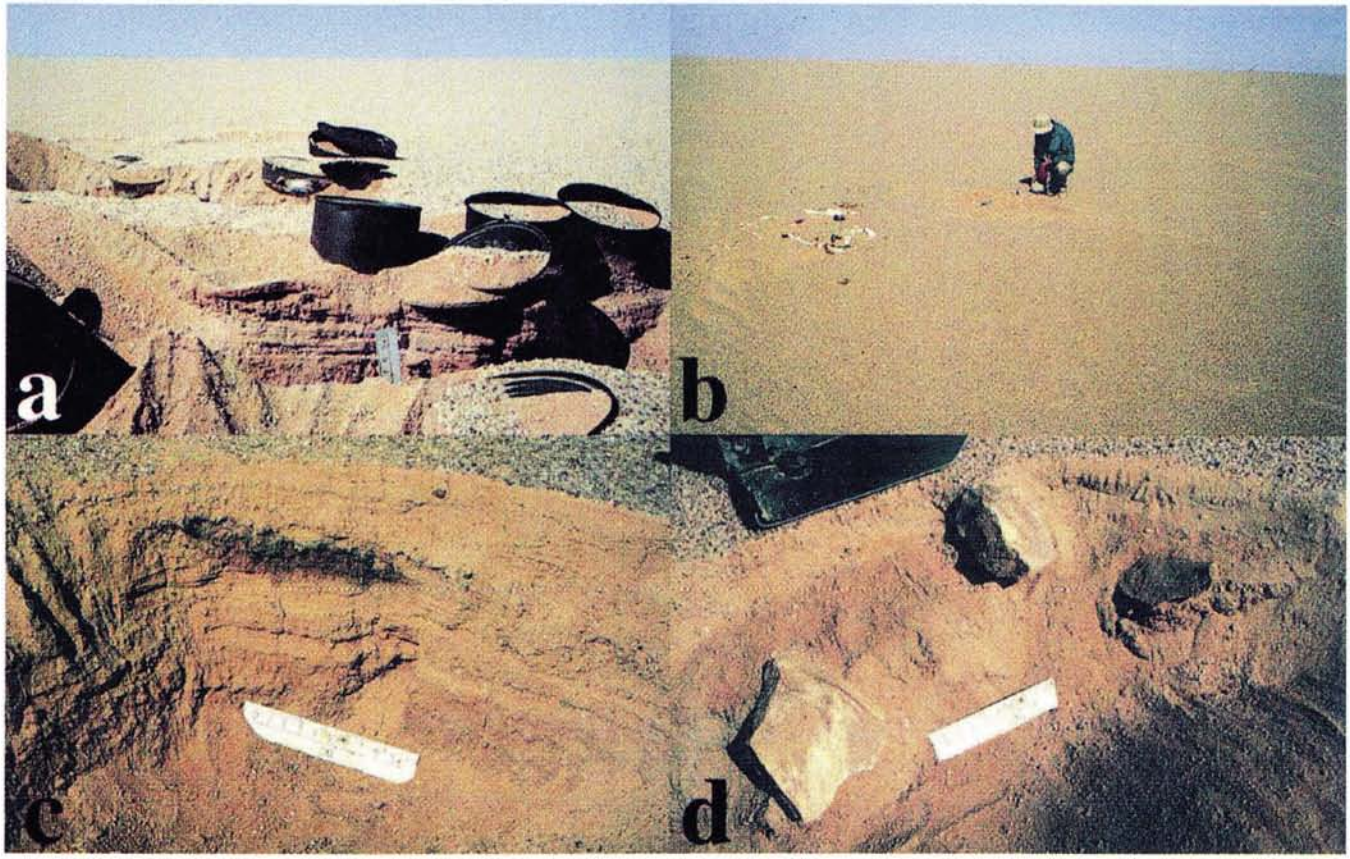

Fig. 14. Artifacts of varying ages in the chevron region: (a) long range desert group camp about 50 km south of the West Line showing sardine and beef tins partially buried by stage 1 sand sheet; (b) location of hearth and camel skeleton east of the North Line; (c) Hearth buried by 3 cm of stage 1 sand sheet (which in turn overlays another 1–3 cm of stage 1 sediment. Hearth was ^{14}C dated at 825 ± 45 bp (AA-11500); (d) Neolithic artifacts (commonly associated with sediments of the latest pluvial at 8–10 kyr) resting on fine pebble alluvium (FPA), with larger implement at top in stage 3 sand sheet. Pit is located at the south end of the North Line.

short-duration rainfall events. In northwest Sudan ~ 250 km south of the Black Hill survey site, Haynes and Johnson (1984) found a buried stage 3 unit overlying stage 1 to 2 units, in turn over a stage 3 paleosol. Thus, the sedimentary influence of the Neolithic pluvial as well as local wetting events make it difficult to associate older stratigraphic sand sheet units with discrete late Pleistocene pluvial events because of the unknown amount of modification during the Holocene.

4. Summary

Observations of the sand sheet at a variety of distances and time scales provide several constraints on theories of formation and modification by water-table stabilization, net deflation and other means. These observations also provide us with the data necessary to determine recent material flux rates and to extrapolate those rates to longer time periods to determine whether they are consistent with the timing of pluvials and rates of denudation for other desert environments. Below, we summarize the observations and measurements of sand sheet units from orbital to ground-based vantage points and present a model for the formation and modification of the near-surface topography and stratigraphy of the Selima Sand Sheet.

The chevron patterns surveyed in the area south of Black Hill are not unique to this area, although their lateral extension is most prominent here as viewed in orbital images. Similar features are also present in discrete, laterally bounded wind streaks that extend down wind from barchan dune fields starting about 3–5 km south of the dune fields, and extending 10–30 km farther to the south until they gradually merge with the surrounding sand sheet. The patterns in both of these settings are visible in all bands of the Landsat MSS and TM images, and can vaguely be seen in the (broad band) color photographs taken by Space Shuttle astronauts. In both color photography and visible bands of electronic sensors, the rest of the sand sheet has extremely little contrast, typically less than 5% reflectance variation, and such patterns are not present. The near-IR

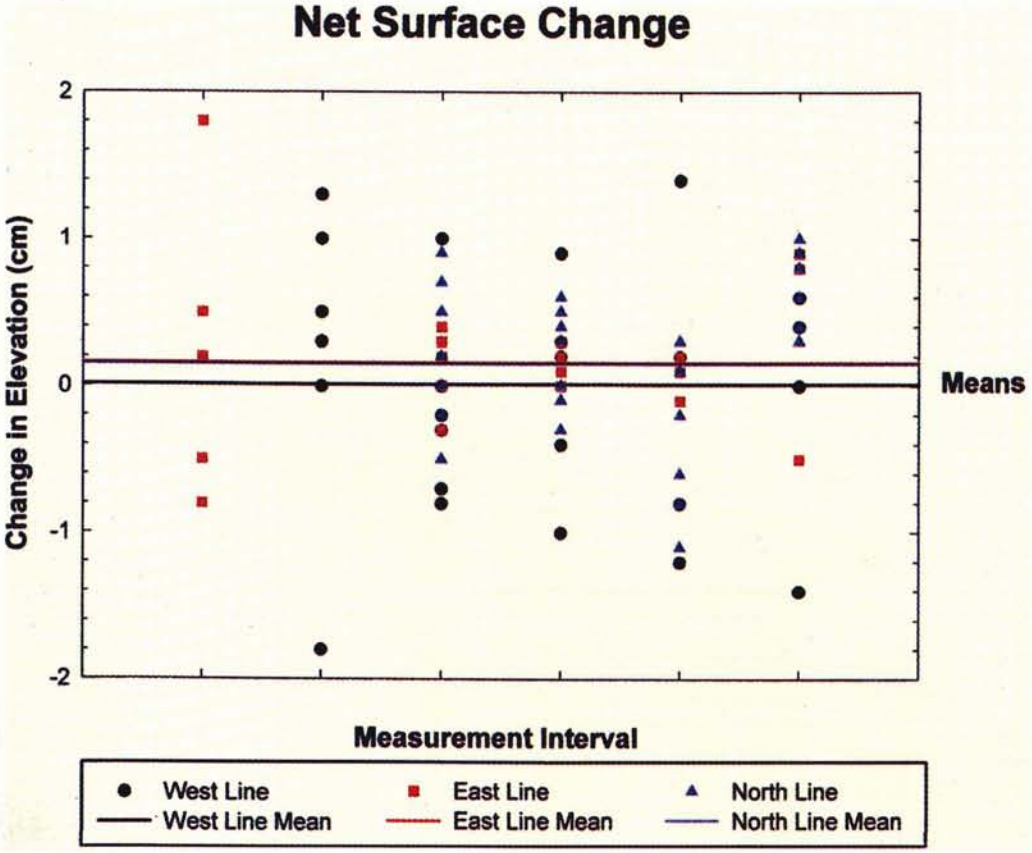

Fig. 15. Summary of surficial elevation changes as measured by the elevation of survey pins. In this plot, each point represents the change in elevation (positive values indicate sedimentation) relative to its last measurement regardless of position on the survey line. Thus, net deposition or erosion would be indicated by values each year clustering above or below the 0-point. The means for each survey line over multiple years indicates no measurable net change that would suggest decadal erosion or deposition.

(Band 7; 2.08–2.35 μm) of the Landsat TM scene does, however, show several transverse chevron-like stripes that are not confined to zones downwind from major topographic obstacles, whose appearance is most likely due to the influence of iron oxides (in the form of grain coatings) on the reflectance in this part of the spectrum. These broad, transverse bright stripes tend to disappear where they impinge on topographically rougher terrain, perhaps because of the break-up of the wind regime (a real effect on sedimentation in those areas) or simply because of a lack of recognition due to the high frequency surface detail in those areas (an observational bias). Although these two possibilities for the absence of chevrons in topographically rough terrain have yet to be tested, the presence of these features in broad areas of the desert indicates that they are not strictly confined to laterally bounded transport zones like barchan dune fields, and that they represent a significant method of sediment transport in other areas of the open desert.

In order to assess sediment transport rates, we rely on the field monitoring measurements presented above. Over the 5 yr of measurements there has been little net change in the surface elevation and thickness of stage 0 exposures. In Fig. 15, a plot of the elevation change measured at each survey pin relative to the last measurement (which shows net change rather than yearly variations at each position on the survey line) indicates that there is virtually no net erosion or deposition. Clusters of points below the 0-point from one set of measurements are matched above the line by similar groups from the next set of measurements, for a net balance of 0. With the exception of a few outlier points, the maximum net change is commonly 1 cm erosion or deposition on each of the lines.

To convert these elevation changes and rates of movement to mass flux, we use a simplified form of Bagnold's (1954, p. 204) equation for sediment transport as used by Haynes (1989). The mass flux per unit area (q given in g/cm s) is the product of the sediment bulk density (γ), rate of advance (c) and height (h), or $q = \gamma ch$, as is customarily applied to dunes. Because the chevrons studied here may not move in a "caterpillar-tread" mode like dunes, this formulation may not be valid in a strict sense, but is included to compare sediment transport flux of chevrons with that of dunes. Using values of 1.6 g/cm^3 for bulk

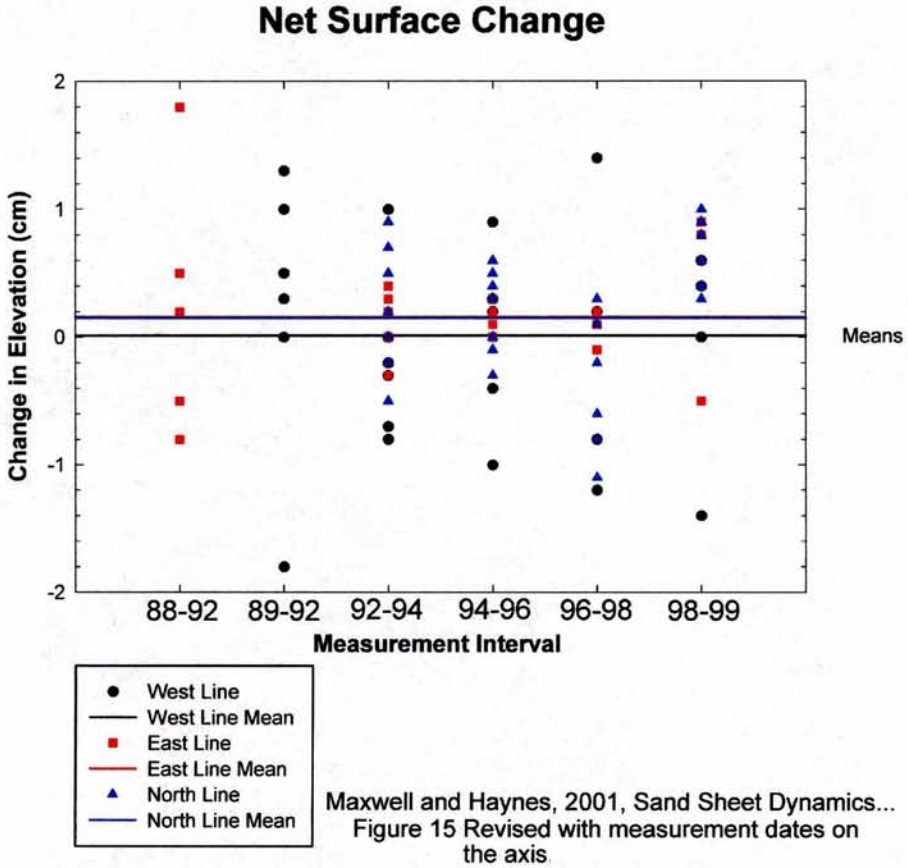

Maxwell and Haynes, 2001, Sand Sheet Dynamics...
Figure 15 Revised with measurement dates on the axis

density and a migration rate of 500 m/yr, a 1-cm thick stage 0 chevron would have a mass flux of 0.0025 g/cm s, or about 25 times less than the 0.064 g/cm s value calculated for a solitary barchan in a field south of the survey area (Haynes, 1989). Since the relation scales linearly, even twice the rate of sand sheet movement (as suggested by the 1986/1988 measurements of the North Line) would increase the flux to only 12 times less than that of dunes. This amount of mass flux seems small compared to that of dunes, but the fact that this flux is spread over 10's of kilometers of the desert floor equates to a much larger net volume transported than that confined to isolated dunes. As is obvious from the stratigraphy present in the survey lines, the sand sheet does not move in a manner similar to dunes, but these estimates illustrate the high rates of movement of sand-sized material based on the rapid transport rate (this estimate does not include the amount of fines that are winnowed by transport).

Such high rates of sediment transport are seemingly at odds with the deposition rates indicated by archaeological and radiometric dating of materials in the sand sheet. The 3-cm burial of the hearth on the North Line dated at 825 yr bp equates to a vertical accretion rate of only 3.7 cm/kyr (although such a steady-state mode of deposition seems highly unlikely in the variable wind regime of the open desert). A much slower long-term rate of deposition is supported by two lines of evidence. First, the stage 1 sediments that overlie this hearth and other archaeological findings are identical in grain size and lamination to stage 0 sediments, and were likely formed by the same processes of granule creep coupled with infilling of fines from suspension. In the short term, the deposits that filled our survey pits from year to year have neither a bimodal distribution nor horizontal lamination (Fig. 4). The fine grain size of those sediments is related to the local depositional environment, since there is little in common between the open sand sheet and a 30 cm pit excavated in the desert floor. Second, where a thick stage 2 sand sheet occurs, OSL dating (20 km east of our survey lines) suggests a net vertical accumulation rate of between 1 and 12 cm/yr (Stokes et al., 1998), but these rates are based on two clusters of ages at 16–21 and 3–4 kyr. Whether sedimentation occurs as a steady-state accumulation or in a more punctuated manner is presently under investigation. These stratigraphic and dating results indicate a much lower rate of vertical accretion than that of horizontal transport, suggesting a model for sand sheet formation that involves significant reworking of sediment. Before considering such a model, however, we must also take into account the ages of formation for the different stages.

Based on the rapid horizontal transport rate of stage 0 sediments and the formation of a stage 1 from stage 0 within historical time, it is likely that a stage 1 sand sheet does not require a significant amount of wetting to produce the admixture of dust and fines necessary to start pedogenesis. Both the strength of the cracking pattern (ped development) and the induration of stage 3 sand sheet deposited at 16–21 kyr (Stokes et al., 1998) indicate that the climate of the Holocene pluvial and even human occupation enabled the disruption of the original sedimentary characteristics. Locally, the stage 3 that overlies the stage 1–2 units near Bagnold's Barchan also was pedogenically altered during the Holocene as judged by Neolithic artifacts inset in the stage 3.

In the absence of cultural remains, the times of deposition and modification of stages 3 and 4 and the FPA and CPG units are more difficult to assign to any discrete age interval. Haynes (1982b (N and S are reversed in Fig. 4 of that reference)) utilized archaeological remains in defining the ages for a three-fold classification of sediments of the Selima Sand Sheet. Intermediate-age alluvium in Wadi Arid with pedogenesis contains Middle Paleolithic artifacts (Haynes, 1985), which by correlation with occurrences elsewhere may be dated at the last interglacial, or 120–150 kyr (Wendorf et al., 1993). At the south end of the sand sheet, red alluvium with stage 4 paleosols has Middle Paleolithic artifacts on its eroded surface (Haynes, 1982b). In the Black Hill region 100 km north of the chevron survey area, alluvium with stage 4 pedogenesis has Acheulian artifacts (Lower Paleolithic) on its eroded surface. The oldest strata in the south (units A and B of Haynes, 1982b) may be equivalent to the FPA of the Black Hill region, and are characterized by exposures of Acheulean artifacts, suggesting an age of > 200 kyr for that surface by correlation with the dating of the Lower Paleolithic in the Bir Tarfawi region (Wendorf et al., 1993). The time of formation and phreatic modification of the CPG is based on Uranium-series dating of the carbonates. The extensive exposures of kunkar that surround Bir Tarfawi and elsewhere in scattered locations have ages ranging from > 350 to 78 kyr (Szabo et al., 1995), but have yet to be traced unequivocally into the more fragmental subsurface sediments of the CPG in the survey line area. Stratigraphically it seems reasonable that the two sediments are equivalent, because nowhere have we found sand sheet units beneath the kunkar, and the CPG sediments where present are always the basal units of our shallow pits. In many cases the pebble-size fragments in the CPG grade into larger size fractions with depth.

In summary, these observations suggest a short-term (10's of years) system of dynamic equilibrium with the sediment supply matched by rapid transport across the sand sheet, and a long-term (100's of years) slow vertical accretion controlled by the geometry of the long wavelength ripples. The presence of stages 1 and 2 sediments on the lee side of the giant ripples and the undulations of the buried upper contacts of stages 3 and 4 further indicate that similar processes of erosion and redeposition have been operating on a 1000-yr time scale. We present below a model for sand sheet evolution that

takes into account these multitemporal observations as well as the changing climate that has modulated the efficiency of aeolian and pedogenic processes.

The record of late Pleistocene hyperaridity punctuated by increasingly shorter intervals of savanna environments argues against a water-table control over the Holocene deposits of the Selima Sand Sheet. However, the kunkar deposits surrounding Bir Tarfawi (see Fig. 2 in Szabo et al., 1995and Fig. 38-1 in Wendorf et al., 1993) do suggest more extensive lacustrine deposits during the middle Pleistocene, although the question of initial water-table control by surface water precipitation of limestone versus remobilization of carbonate by a shallow water table is not resolved. Pachur et al. (1987) used the term "phreatogenic crusts" to describe calcareous crusts that occur in many shallow depressions in southern Egypt and northern Sudan, and interpreted them as resulting from a regional rise in the groundwater table. Because of the remobilization by later groundwater, such material may not always yield consistent dates except in local depositional environments (Röper, 1993; Szabo et al., 1995). The fact that CPG is not ubiquitous in the sand sheet could be due to local erosion of pre-existing deposits as well as non-deposition (supported by the undulatory top contacts of the CPG and FPA in our survey lines), leaving open the question of a middle Pleistocene lacustrine or high water-table environment.

Our model for the origin of the northern part of the sand sheet begins with a middle Pleistocene alluvium and carbonate-cemented fine gravel. During at least three mid-Pleistocene pluvials at ~320–250, 240–190 and 155–120 kyr (Szabo et al., 1995) scattered ponding and localized runnels were the likely cause of the initial shallow topography on the alluvial surface. The importance of aeolian recycling and ripple migration began with the increased length and severity of the arid periods during the late Pleistocene. The oldest sand sheet sediments of the core of the Selima Sand Sheet were likely deposited during the arid periods of the mid-Pleistocene, and owe their initial pedogenic modification (to stage 4) to the intervening pluvials. Locally, the stage 3 unit from Bagnold's Barchan region indicates that not all stage 3 pedogenesis resulted from a single pluvial period. In the central part of the sand sheet, these older aeolian deposits infilled local low areas of the fluvially dissected CPG and FPA, and created a quasi-planar surface that was stabilized during the pluvial of either the last interglacial (155–120 kyr) or that of ^{18}O substages 5c or 5a (90–65 kyr). Here, the gently undulating erosional surface of the middle Pleistocene or older alluvium provided the initial topographic irregularity that led to accumulation and preservation of younger sand sheet sediments on the lee side of shallow ripples.

Both archaeological evidence for the lack of Upper Paleolithic habitation (Wendorf et al., 1993) and radiometric dating of carbonates (Szabo et al., 1995) indicate that the period from 65 to ~12 kyr was extremely arid in this part of the Sahara. It is this time period that likely was responsible for extensive deposition of sand sheet (dated at 21–16 kyr, Stokes et al., 1998). These deposits were then stabilized by the semiarid climate of the Holocene pluvial (ca: 10-6 kyr) on an undulatory surface that set the stage for the present cycle of sand sheet deposition. The wetting cycles of this "Neolithic" pluvial converted upper portions of late Pleistocene sand sheet sediments to stage 3 as Neolithic pastoralists occupied the region. Subsequent rainfall events formed prismatic desiccation patterns in the sand sheet resulting in stage 2 paleosols. The brief intervals did not, however, provide enough time, rainfall or biologic activity to disrupt the dominant horizontal stratification of the near-surface deposits. The end of the Neolithic pluvial saw resumption of hyperarid sedimentation resulting in the stage 1 and 0 deposits. Stage 1 units have been formed from the stage 0 within time spans of 10's of years, but have not yet been subjected to major pluvial activity that would more completely modify their internal structure by pedogenic processes. Stage 0 sediments continue to migrate across these gentle ripples rooted in the earlier topography, repeatedly exposing older stages that contain darker granules due to more pronounced iron coatings making the patterns visible with orbital sensors.

5. Discussion

This scenario for the evolution of the sand sheet adds a degree of complexity to other models that have been proposed for sand sheets in North America (Kocurek and Nielson, 1986) and for the Selima Sand Sheet itself (Peel, 1966; Haynes, 1982b). In summarizing the environments of six modern sand sheets, Kocurek and Nielson (1986) found five factors that contribute to sand sheet formation: (1) a high water table, (2) surface cementation, (3) periodic flooding, (4) a significant coarse-grained sediment population, and (5) vegetation. Discounting the hydrologic factors that obviously do not apply to the hyperarid late Pleistocene and Holocene history of the Selima Sand Sheet, we are left with an origin aided by the presence of the proper particle sizes; those too large to allow dune formation, but not coarse enough to completely inhibit sediment reworking. While we agree that the granule coating (Maxwell, 1982) can sustain and even nurture the present-day sand sheet, we prefer to decouple the origin of the paleo-surfaces underlying these sediments from that of the sand sheet deposits themselves. Sandford (1933), in fact, seems to have recognized this distinction for the Selima Sand Sheet long ago. He advocated a two-fold division of low relief surfaces into desert peneplains or surfaces of maximum denudation,

versus the sand sheet, which he interpreted to represent regions of net accumulation of sand. A more dynamic classification of such surfaces is provided by the concept of bounding surfaces (Kocurek, 1991, 1998), with the present surface of the Selima Sand Sheet representing the ultimate super bounding surface.

The area studied here differs greatly from the North American sand sheets and interdune deposits whose descriptions are prevalent in the literature (Folk, 1968; Fryberger et al., 1979; Kocurek and Nielson, 1986; Nielson and Kocurek, 1987; Kocurek et al., 1992) due to its size, setting, longevity, climate and widespread lack of relief. Typical interdune deposits within dune fields may cover a few thousand square meters, versus the tens of thousands of kilometers in southern Egypt. The geologic setting upon Cretaceous and younger friable sandstones provides a widespread ample source of sand as well as iron, and the lack of relief cannot be overstated. In addition, some of the sand sheet deposits studied here have been in situ since at least the middle Pleistocene, as opposed to more transient interdune zones that may experience rapid burial or exposure. Thus, we view the origin of this sand sheet as largely due to inheritance of an area of initially low relief due to the near horizontal bedrock, and fluvial activity during the middle to late Tertiary that eroded the once overlying limestones and shales of the retreating early Tertiary sea (Issawi and McCauley, 1992). Climatic shifts likely played a part in the late Tertiary history, continually reducing high points, and depositing sand with a lag surface during the intervening arid intervals. Such deposits could well have been more difficult to erode than the intervening patches of sedimentary bedrock. As relief was reduced, the broad alluvial channels were likely armored from aeolian erosion by lag deposits, and the thalwegs became the central axes for inverted wadis, whose gravel spreads are still distinct today at the margins of the sand sheet.

The model for sand sheet evolution presented above is based largely on measurements and observations in the now hyperarid core of the Selima Sand Sheet. However, the geographic extent to which this model applies may be limited. Haynes and Johnson's (1984) observation of stage 3 sediments overlying a stage 1–2 at the south end of the sand sheet suggests that not all the stage 3 resulted from enhanced rainfall of the Holocene. Pedogenesis in this area may have resulted from multiple wet periods within the Neolithic pluvial with intervening dry periods. Within the core of the Darb el-Arba'in Desert, however, such stratigraphic relations have not been found. Perhaps at the margins of the sand sheet, where climate-forced changes are likely to be more severe, the chronologic significance of the different stages may break down. Further dating and stratigraphic observations are obviously needed to test the geographic extent of this model and the chronologic significance of the stages. If we depend on stratigraphic arguments alone, it is possible that local wetting conditions in different parts of the sand sheet would lead to modification at different times; thus we could be mistaking local rain and/or ponding for a regional climatic effects. Nonetheless, even if the exact ages are incorrect, the stratigraphic evidence for initial alluvial surface, aeolian deposition, stabilization and repeated deposition is hard to discount, and provides insight into process of arid landscape response under changing climate.

Finally, even with the problems involved in dating early and middle Pleistocene geomorphic features, it is possible to test this model for the development of the sand sheet. Optically stimulated luminescence dating is providing the first record of deposition during the arid phases in this part of the desert (Stokes et al., 1998), and we have obtained detailed samples of stage 2 (and older) sand sheets to determine their rate of aggradation. Further dating of carbonates can provide a test for the extent of lacustrine deposition during pluvial periods, but is also subject to interpretation because of a shallowing of the groundwater table during wet periods that may not necessarily tie into major pluvial events. Talbot (1985) proposed a variant of the water-table control, suggesting that the primary effect of a high water table would be to stabilize the surface with vegetation. It will be difficult to test whether the original pre-sand sheet surface was controlled by the water table that aided calcification of the CPG. The topography on the buried surface of the CPG is so poorly known that it is presently impossible to estimate a presumed water table. In addition, localized groundwater within fluvial paleochannels further complicate mapping of the water table relative to pre-existing topography. Nonetheless, additional stratigraphic test pits will help us refine ideas on the extent of the basal units of the sand sheet and their role in creating the present surface.

5.1. Implications for quaternary landscape development

Both the interpretation of an initial low-relief surface that set the stage for sand sheet deposition, and the multitemporal monitoring results that indicate dynamic equilibrium rather than net aggradation during hyperarid intervals influence our ideas of the long-term development of the Quaternary landscape of southern Egypt. In particular, the origin of the paleo-surface that was later to become the Selima Sand Sheet bears directly on the late Tertiary history of southern Egypt. The role of climate in creating and preserving relict sand sheet sediments and the presence of buried topography (McCauley et al., 1982) suggest a more complex origin for this landscape than simple aeolian peneplanation. Sandford (1933) suggested that two erosional surfaces were present in this region: that of the Gilf Kebir plateau, located 100 km west of the detailed survey area, and that of the

sand sheet. According to Sandford (1933), both of these surfaces are controlled by bedrock. However, the presence of deep incised wadis in the Gilf Kebir (Peel, 1939; Maxwell, 1980) and the now-buried channels in the sand sheet (McCauley et al., 1982) suggest a pre-existing surface of fluvial dissection rather than one of planed bedrock. In addition to these channels, 200 km to the east of the sand sheet, relict incised drainage is now exposed on the surface of the limestone plateau. Unlike the deeply incised wadis of the Gilf Kebir, one of these channels (Wadi Mareef) extends for over 50 km into the central part of the plateau, and changes width abruptly where lakes once were formed by dammed portions of the channels.

The fluvial dissection that eroded the early Tertiary deposits in southern Egypt was largely completed prior to the onset of Quaternary climatic cycling, as suggested by several lines of geomorphic evidence. Said (1980, 1983) pointed to the occurrence of gravel spreads north of the sand sheet and a hypothetical distribution of Eocene–Oligocene drainage that debouched to the north as evidence that the mid-Tertiary stream systems were responsible for much of the denudation of the southern part of the desert. McCauley et al. (1982) documented the occurrence of drainage in this region revealed by the SIR-A experiment, which showed NE-SW aligned stream channels at the border of Egypt and Sudan interpreted to represent fluvial denudation as old as mid-Tertiary. The direction of drainage beneath the sand sheet led McCauley et al. (1986) to postulate the occurrence of a "Trans-African drainage system" or "TADS," composed of mid-Tertiary drainage that flowed from east to west across what is now southern Egypt and northern Sudan. Such a hypothesis has not gone unchallenged. Burke and Wells (1989) provided several lines of evidence that instead of flowing westward across Africa, these ancient channels more likely turned to the south and were tributaries to the northeast flowing Wadi Howar in northern Sudan (Pachur and Kropelin, 1987). Finally, Issawi and McCauley (1992) combined results from SIR-A and B, which they interpreted to support the TADS hypothesis, with the problem of the acute, southward facing tributaries (Wadi Qena) to the Nile, and synthesized much of the fluvial history of southern Egypt. According to their work, mid-Tertiary drainage flowed westward across southern Egypt, turning to the north in the area of the sand sheet. Despite the disputed outflow direction of the radar-detected channels, and the details of timing within the broad constraints of the mid-Tertiary, it is apparent that fluvial activity was paramount in the initial etching of the Selima Sand Sheet. However, additional observations also suggest that drainage was not totally responsible for the final configuration of the pre-Quaternary, low-relief landscape. Those channels visible in the SIR-A and B images are not meandering as would be expected from the penultimate stage of fluvial dissection, but are straight, which may in part be due to structural control by the ENE fracture system of the region (Issawi, 1971). In addition, the margins of the radar-detected channels protrude above even the present surface of the sand sheet, making portions of them visible in enhanced Landsat images of the region (Davis et al., 1993). Thus, even by the end of the primary fluvial sculpture in the late Tertiary, there was more relief in this region than would be expected from an alluvial plain. Consequently, the problem of denudation remains, and particularly why it was concentrated in the region between the Gilf Kebir and the limestone plateau (Fig. 1).

In discussing the origin of the low-relief surfaces and neighboring escarpments in southern Egypt (and elsewhere), Higgins (1990) advocated extensive scarp retreat as the primary mechanism for forming the lower level (sand sheet) surface of Sandford. In fact, scarp retreat was also advocated for the high cliffs of the Gilf Kebir plateau (Peel, 1939) and for the enlargement of wadis within the plateau itself (Maxwell, 1980). However, whether such a process can be invoked for denudation across hundreds of kilometers over time periods of a few million years is hindered by both the lack of (now eroded) evidence and the high rates of cliff retreat that would be required.

An alternative to the individual processes of fluvial denudation or scarp retreat is suggested by the aggradation and dynamic equilibrium forced by climatic cycling during the late Tertiary and Quaternary (deMenocal, 1995; Lancaster, 1998). Over the Tertiary, it is likely that fluvial erosion prevailed, but with the onset of Quaternary climate change, landscape modification became increasingly dominated by periods of aeolian erosion and deposition, and stabilization of the land surface during increasingly brief pluvials. During periods of hyperaridity, interfluves were stripped by aeolian erosion, while deposition was confined to local topographically controlled zones. With increased rainfall, those aeolian deposits were likely stabilized by vegetation, and fluvial erosion enhanced by weathering and pedogenesis further reduced topography by erosion of bedrock highs. As these cycles continued into the late Pleistocene, the effects of aeolian resurfacing and protection of zones of accumulation by both vegetation during pluvials and armoring by coarse grains during arid intervals made the region ripe for topographic inversion (Haynes, 1985). Such a sequence could have been accentuated by the flux of material eroded from the Great Sand Sea.

Rather than extensive cliff retreat of the Gilf Kebir to the west and the limestone plateau to the east, it is possible that the aeolian setting of the sand sheet aided denudation of the Darb el-Arba'in Desert. The Selima Sand Sheet lies directly downwind of the Great Sand Sea, which provides a source of sediments for infilling the paleo-topography as well as for eroding grains from the Nubian sandstone (Haynes, 1989). In contrast, the

limestone plateau lies downwind from Pliocene gravels more than 500 km to the north–northwest. Evidence for sand transport here lies only on the downwind end of the plateau where scattered longitudinal dunes form in topographically controlled settings. Thus, the plateau acts as a major sand transport zone, with little accumulation on the surface itself. The surface of the Gilf Kebir is similar in that aeolian deposits are only present as isolated dunes controlled by the abrupt topography of the wadis. Thus, at least over the middle and late Pleistocene, these plateaus were dominated by transport during arid periods rather than aggradation. In contrast, the sand sheet cycles of aeolian aggradation and erosion, topographic inversion, and sporadic fluvial erosion may well have become a positive feedback system that continues to the present day.

6. Conclusions

Monitoring the sand sheet through the use of repeated remote sensing and field surveys has resulted in new constraints on models for the formation of this vast expanse of mobile sand and on the geomorphic development of the southwestern desert of Egypt in the late Tertiary and Quaternary. Changes seen in multi-year Landsat images are on the order of 2–4% reflectance, but in this area of uniform topography, are enough to delineate large-scale movement in the sand sheet. Chevrons move at rates of 500–1000 m/yr in the present environment and are made up of 5–1 cm thick units of active sand sheet. Typically, 0–2 cm of active sand sheet are eroded or deposited along the three survey lines that we have monitored. These patterns are caused by the erosion of the darker, coarse admixture of older sand sheet units that have a greater coating of iron oxides. The most active strata of the sand sheet are deposited in the lee of the modern low amplitude ripples, and translate downwind (south) in a progradational mode much like ripples of more normal sizes. Sand transport rates and thickness estimates for these features suggest a mass flux that is much less per unit width than that of dunes, but which may occur over vast expanses of southwestern Egypt. Chevrons have only been documented in areas of uniform reflectance where the 'noise' of surface features does not interfere with the recognition of minor reflectance variations.

In contrast to these high volumes of sediment transport, longer-term observations of the remains of Sudan Defense Force camps indicate little net erosion, and in some instances, burial of deposits and formation of slightly indurated sand sheet sediments between 1942 and the present. The depth of burial of archaeological materials and OSL dating suggest accumulation rates of < 1–12 cm/yr for the sand sheet, but whether this sedimentation is a steady state, or a more stochastic process is not yet defined. Reconciliation of the high mass movement with such small accumulation rates suggests that the sand sheet is now in a state of dynamic equilibrium, with the net influx of sediment from upwind as well as local contributions roughly equal to the transport out of the system.

Stratigraphic investigations along the survey lines as well as elsewhere in the sand sheet indicate that the older stages of sand sheet sediments, those that show significant pedogenesis, were likely deposited during the hyperarid intervals of the middle to late Pleistocene, whereas those that have lost their horizontal lamination (stage 3) were likely deposited prior to the Neolithic pluvial of the early Holocene. These latter sediments retain an undulating surface that was likely stabilized during that wet period, and formed the topographic setting used for later hyperarid-period aggradation of the sand sheet. Still older alluvial units (FPA and CPG) likewise have an undulating surface, suggesting that if a paleo-water table controlled the initial topography, it was extensively eroded prior to deposition of the oldest sand sheet units. A net aggradational origin for the Selima Sand Sheet is not supported by these observations and multi-year measurements, nor is a total degradational origin. Climatic variations during the Quaternary resulted in alternating periods of sand sheet deposition and stabilization, leading to infilling of local lows, erosion of protruding bedrock, and consequent topographic inversion. The present- day hyperarid climate is dominated by low rates of sedimentation in the lee of low-amplitude ripples, similar to the older sand sheets of the late Pleistocene.

The distribution and local topographic undulations of the alluvial sediments beneath the sand sheet as well as the topographic variations of the local bedrock suggest that the initial surface of the sand sheet was not the denudational plain envisioned by early workers. Instead, the decline of fluvial dominance at the end of the Tertiary led to an irregular landscape that was influenced by climatic variations of the Quaternary. A combination of the initial fluvial landscape inherited from Tertiary erosion, and climatic cycling during the Quaternary resulted in the formation of the low-relief aeolian surface that we know today as the Selima Sand Sheet.

Acknowledgements

This research has been supported by grants from the National Geographic Society and NSF Grant EAR 8607479 to C.V. Haynes (1986–1991), by NASA Grant NAGW-3711 to T.A. Maxwell (1992–1996), and by the Walcott and Becker Funds of the Smithsonian Institution. Long-standing help and expertise in the geomorphology of southern Egypt has been provided by Bahay Issawi of the Ministry of Mines and Mineral Industries,

and Gaber Naim and Mohamed Hinnawi of the Egyptian Geological Survey and Mining Authority. Early Phases of this work were aided Hassan El-Etr and Nabil Embabi of Ain Shams University and by Mohamed Askalany of Asyut University. For assistance in field research and discussions of the sand sheet we are grateful for the help of Keith Katzer, Bill Gillespie, Stephen Stokes, Kathleen Nicoll, and Peter Patton. Ali Hawari and Ali Kilani were valuable liaisons with the Egyptian Geological Survey, and provided excellent field assistance. Analysis of the remote sensing data was supported by Andrew Johnston, Kathleen Nicoll, Chris Swezy, and especially Becky Jauquet who spent three summers re-registering and correcting much of the Landsat data. We thank Mary Bourke, Gary Kocurek, and Nick Lancaster for detailed and helpful reviews of the manuscript.

References

Bagnold, R.A., 1954. The Physics of Blown Sand and Desert Dunes. Methuen and Co., London, 265 p.

Bagnold, R.A., 1990. Sand Wind and War: Memoirs of a desert explorer. Univ. Arizona Press, Tucson, 209 pp.

Breed, C.S., McCauley, J.F., Grolier, M.J., 1982. Relict drainage, conical hills and the eolian veneer in southwest Egypt—application to Mars. Journal of Geophysical Research 87, 9929–9950.

Breed, C.S., McCauley, J.F., Davis, P.A., 1987. Sand sheets of eastern Sahara and ripple blankets on Mars. In: Frostick, L., Reid, I. (Eds.), Desert Sediments Ancient and Modern. Geological Society Special Publication, Vol. 35, London, pp. 337–359.

Burke, K., Wells, G.L., 1989. Trans-African drainage systems of the Sahara: Was it the Nile?. Geology 17, 743–747.

Davis, P.A., Breed, C.S., McCauley, J.F., Schaber, G.G., 1993. Surficial geology of the Safsaf region, south-central Egypt, derived from remote sensing and field data. Remote Sensing Environment 46, 183–203.

deMenocal, P.B., 1995. Plio-Pleistocene African climate. Science 270, 53–59.

El-Baz, F., Maxwell, T.A. (Eds.), 1982. Desert landforms of southwest Egypt: a basis for comparison with Mars. Washington, NASA CR-3611, 372 p.

El-Baz, F., Boulos, L., Breed, C., Dardir, A., Dowidar, H., El-Etr, H., Embabi, N., Grolier, M., Haynes, V., Ibrahim, M., Issawi, B., Maxwell, T., McCauley, J., McHugh, W., Moustafa, A., Yousif, M., 1980. Journey to the Gilf Kebir and Uweinat, Southwest Egypt, 1978. Geographical Journal 146, 51–93.

Folk, R.L., 1968. Bimodal supermature sandstones: product of the desert floor. In International Geological Congress: Report of the 23rd Session, Chekoslovakia, Academia, Prague, pp. 9–32.

Folk, R.L., 1971. Longitudinal dunes of the northwestern edge of the Simpson Desert, Northern Territory, Australia. 1. Geomorphology and grain size relationships. Sedimentology 16, 5–64.

Fryberger, S.G., Ahlbrandt, T.S., Andrews, S., 1979. Origin, sedimentary features and significance of low-angle eolian sand sheet deposits, Great Sand Dunes National Monument and vicinity, Colorado. Journal of Sedimentary Petrology 49, 733–746.

Haynes, Jr., C.V. 1982a. The Darb El-Arba'in Desert: A product of quaternary climatic change. In: El-Baz, F., Maxwell, T.A. (Eds.), Desert Landforms of Southwest Egypt: A basis for Comparison with Mars. NASA CR-3611, Washington DC, 372 p.

Haynes Jr., C.V., 1982b. Great sand sea and Selima Sand Sheet, Eastern Sahara: Geochronology of Desertification. Science 217, 629–633.

Haynes Jr., C.V., 1985. Quaternary studies, Western Desert, Egypt and Sudan 1979–1983 Field Seasons. National Geographical Society of Research Reports 16, 269–341.

Haynes Jr., C.V., 1987. Holocene migration rates of the Sudano-Sahelian Wetting Front, Arba'in Desert, Eastern Sahara. In: Close, A.E. (Ed.), Prehistory of Arid North Africa. SMU Press, Dallas, pp. 69–84.

Haynes Jr., C.V., 1989. Bagnold's Barchan: A 57-Yr record of dune movement in the Eastern Sahara and implications for dune origin and paleoclimate since Neolithic times. Quaternary Research 32, 153–167.

Haynes Jr., C.V., Eyles, C.H., Pavlish, L.A., Ritchie, J.C., Rybak, M., 1989. Holocene Paleoecology of the Eastern Sahara; Selima Oasis. Quaternary Science Reviews 18, 109–136.

Haynes Jr., C.V., Haas, H., 1980. Radiocarbon evidence for Holocene recharge of groundwater, Western Desert, Egypt. Radiocarbon 22, 705–717.

Haynes Jr., C.V., Johnson, D.L., 1984. A provisional soil chronosequence for the Quaternary of the Eastern Sahara. Geological Society of American Abstracts with Programs 16, 534–535.

Haynes Jr., C.V., Maxwell, T.A., Johnson, D.L., 1993. Stratigraphy, geochronology, and origin of the Selima Sand Sheet, eastern Sahara, Egypt and Sudan. In: Thorweihe, U., Schandelmeier, H. (Eds.), Geoscientific Research in Northeast Africa. A. A. Balkema, Rotterdam, pp. 621–626.

Haynes, Jr., C.V. Mehringer, Jr., P.J. El Sayed Abbas Zaghloul, 1979. Pluvial lakes of northwestern Sudan. Geographical Journal 145, 437–445.

Higgins, C.G., 1990. Chapter 14, Seepage-induced cliff recession and regional denudation with case studies by Osterkamp, W.R. and Higgins, C.G. In: Higgins, C.G., Coates, D.R., (Eds.), Groundwater Geomorphology; The Role of Subsurface Water in Earth-surface Processes and Landforms. Boulder, Colorado, Geological Society of America Special Paper 252.

Issawi, B., 1971. Geology of the Darb El Arba'in, Western Desert. Annals of the Geological Survey of Egypt 1, 53–92.

Issawi, B., 1972. Review of upper Cretaceous–lower Tertiary stratigraphy in central and southern Egypt. American Association of Petrolium Geological Bulletin 56, 1448–1463.

Issawi, B., McCauley, J.F., 1992. The Cenozoic rivers of Egypt: the Nile problem. In: Hoffmann, A., Friedman, R., Adams, B. (Eds.), The Followers of Horus: Studies in Memory of Michael. Oxbow Press, Oxford, England, pp. 121–138.

Kocurek, G., 1991. Interpretation of ancient eolian sand dunes. Annual Review of Earth and Planetary Science 19, 43–75.

Kocurek, G., 1998. Aeolian system response to external forcing factors—A sequence stratigraphic view of the Saharan region. In: Alsharhan, A.S., Glennie, K.W., Whittle, G.L., Kendall, C.G.St.C. (Eds.), Quaternary Deserts and Climatic Change. A.A. Balkema, Rotterdam and Brookfield VT, pp. 327–337.

Kocurek, G., Nielson, J., 1986. Conditions favourable for the formation of warm-climate aeolian sand sheets. Sedimentology 33, 795–816.

Kocurek, G., Townsley, M., Yeh, E., Havholm, K., Sweet, M.L., 1992. Dune and dune-field development on Padre Island, Texas, with implications for interdune deposition and water-table-controlled accumulation. Journal of Sedimentary Petrology 62, 622–635.

Lancaster, N., 1998. Dune morphology, chronology and Quaternary climatic change. In: Alsharhan, A.S., Glennie, K.W., Whittle, G.L., Kendall, C.G.St.C. (Eds.), Quaternary Deserts and Climatic Change. A.A. Balkema, Rotterdam and Brookfield VT, pp. 339–349.

Machette, M.N., 1985. Calcic soils of the southwestern United States. In: Weide, D.L. (Ed.), Soils and Quaternary Geology of the Southwestern United States. Geological Society of America Special Paper, Vol. 203, pp. 1–21.

Markham, B.L., Barker, J.L., 1986. Landsat MSS and TM post-calibration dynamic ranges, exoatmospheric reflectances and at-satellite

temperatures. Landsat Technical Notes, No. 1, Eosat, Lanham MD, pp. 3–8.

Maxwell, T.A., 1980. VII. Geomorphology of the Gilf Kebir. in Journey to the Gilf Kebir and Uweinat, Southwest Egypt, 1978. Geographical Journal 146, 51–93.

Maxwell, T.A., 1982. Sand sheet and lag deposits in the southwestern desert. In: El-Baz, F., Maxwell, T.A. (Eds.), Desert Landforms of Southwest Egypt: A Basis for Comparison with Mars. NASA, Washington DC, pp. 157–174.

Maxwell, T.A., Haynes, C.V., 1989. Large-scale, low-amplitude bedforms (Chevrons) in the Selima Sand Sheet, Egypt. Science 243, 1179–1182.

Maxwell, T.A., Haynes, C.V., 1992. Remote sensing of sand transport in the Western Desert of Egypt. In: Sadek, A. (Ed.), Geology of the Arab World. Cairo Univ. Press, Cairo, Egypt, pp. 19–31.

McCauley, J.F., Breed, C.S., Schaber, G.G., McHugh, W.P., Haynes, C.V., Grolier, M.J., El-Kilani, A., 1986. Paleodrainages of the eastern Sahara, the radar rivers revisited (SIR-A/B implications for a mid-Tertiary trans-Africa drainage system). IEEE Transactions on Geoscience and Remote Sensing GE-24, 624–648.

McCauley, J.F., Schaber, G.G., Breed, C.S., Grolier, M.J., Haynes, C.V., Issawi, B., Elachi, C., Blom, R., 1982. Subsurface valleys and geoarchaeology of the eastern Sahara revealed by shuttle radar. Science 218, 1004–1020.

McFadden, L.D., Wells, S.G., Jercinovich, M.J., 1987. Influences of eolian and pedogenic processes on the origin and evolution of desert pavements. Geology 15, 504–508.

McHugh, W.P., McCauley, J.F., Haynes, C.V., Breed, C.S., Schaber, G.G., 1988. Paleorivers and geoarchaeology in the southern Egyptian Sahara. Geoarchaeology 3, 1–40.

McHugh, W.P., Schaber, G.G., Breed, C.S., McCauley, J.F., 1989. Neolithic adaptation and the Holocene functioning of Tertiary Paleodrainages in southern Egypt and northern Sudan. Antiquity 63, 320–336.

Nielson, J., Kocurek, G., 1987. Surface processes, deposits, and development of star dunes: Dumont dune field, California. Geological Society of American Bulletin 99, 177–186.

Pachur, H.J., Kropelin, S., 1987. Wadi Howar: paleoclimatic evidence from an extinct river system in the southeastern Sahara. Science 237, 298–300.

Pachur, H.-J., Röper, H.-P., Kröpelin, S., Goschin, M., 1987. Late Quaternary hydrography of the Eastern Sahara. Berliner Geowiss. Abh. 75 (2), 331–384.

Peel, R.F., 1939. The Gilf Kebir: Part 4 in Bagnold, R.A. and others, an expedition to the Gilf Kebir and Uweinat, 1938. Geographical Journal 93, 295–307.

Peel, R.F., 1966. The landscape in aridity. Institute of British Geographers Transactions 38, 1–23.

Ritchie, J.C., Eyles, C.H., Haynes Jr., C.V., 1985. Sediment and pollen evidence for an early to mid-Holocene humid period in the eastern Sahara. Nature 314, 352–355.

Röper, H.-P., 1993. Calcretes in the Western desert of Egypt. In: Thorweihe, U., Schandelmeier, H. (Eds.), Geoscientific Research in Northeast Africa. Balkema, Rotterdam, pp. 635–639.

Said, R., 1980. The Quaternary sediments of the southern western desert of Egypt: an overview. In: Wendorf, F., Schild, R. (Eds.), Prehistory of the Egyptian Sahara. Academic Press, New York, 414 p.

Said, R., 1983. Remarks on the origin of the landscape of the eastern Sahara. Journal of African Earth Sciences 1, 153–158.

Said, R. (Ed.), 1990. The Geology of Egypt. A.A. Balkema, Rotterdam, 734 p.

Said, R., 1993. The River Nile: Geology, Hydrology and Utilization. Pergamon Press, New York, 320 p.

Sandford, K.S., 1933. Geology and geomorphology of the southern Libyan Desert. In: Bagnold, R.A.(Ed.), A Further journey through the Libyan Desert Con't. Geographical Journal 82, 213–219.

Stokes, W.L., 1968. Multiple parallel truncation bedding planes—a feature of wind-deposited sandstone formations. Journal of Sedimentary Petrology 38, 510–515.

Stokes, S., Maxwell, T.A., Haynes Jr., C.V., Horrocks, J.L., 1998. Latest Pleistocene and Holocene sand-sheet construction in the Selima Sand Sea, Eastern Sahara. In: Alsharhan, A.S., Glennie, K.W., Whittle, G.L., Kendall, C.G.St.C. (Eds.), Quaternary Deserts and Climatic Change. AA Balkema, Rotterdam and Brookfield VT, pp. 175–183.

Szabo, B.J., Haynes Jr., C.V., Maxwell, T.A., 1995. Ages of Quaternary pluvial episodes determined by uranium-series and radiocarbon dating of lacustrine deposits of Eastern Sahara. Palaeogeography, Paleoclimatology, Palaeoecology 113, 227–242.

Talbot, M.R., 1985. Major bounding surfaces in aeolian sandstones—a climatic model. Sedimentology 32, 257–265.

Wendorf, F., Schild, R., 1980. Prehistory of the Eastern Sahara. Academic Press, New York, 414 p.

Wendorf, F., Schild, R., Said, R., Haynes, C.V., Gautier, A., Kobusiewicz, M., 1976. The Prehistory of the Egyptian Sahara. Science 193, 103–114.

Wendorf, F., Schild, R., Close, A.E., 1993. Summary and conclusions, pp. 552–573. In: Egypt during the last Interglacial, The Middle Paleolithic of Bir Tarfawi and Bir Sahara East. Wendorf, F., Schild, R., Close A.E. and Associates (Eds.), Plenum Press, New York, 596 p.

Wright, J.W., 1945. War-time exploration with the Sudan defence force in the Libyan desert 1941–1943. Geographical Journal 105, 100–111.